Lipid signaling and inflammation: metabolomics for better diagnosis and treatment strategy

Yang, W.

Chapter II

A comprehensive UHPLC-MS/MS method for metabolomics profiling of signaling lipids: markers of oxidative stress, immunity and inflammation

Based on:

Wei Yang, Johannes C. Schoeman, Lieke Lamont, Yolanda de Rijke, Alireza Mashaghi, Amy C. Harms, Thomas Hankemeier

A comprehensive UHPLC-MS/MS method for metabolomics profiling of signaling lipids: markers of oxidative stress, immunity and inflammation

Manuscript in preparation

Abstract

Signaling lipids (SLs) are of essential importance in diverse biological cascades, containing lipid backbone moieties. Emerging evidence showing the pathophysiological relevance of SLs necessitates their metabolic profiling and biological elucidation while the dramatic differences in endogenous abundances across lipid classes as well as multiple isomers within the same lipid class makes the development of a generic analytical method challenging. In this study, a comprehensive, sensitive and robust ultra-high performance liquid chromatography–tandem mass spectrometry method was developed and validated targeting oxylipins (isoprostanes, prostaglandins and other oxidized lipids), free fatty acids, lysophospholipids, sphingoid bases (C16, C18), platelet activating factors (C16, C18), endocannabinoids and bile acids. The validated method was successfully applied for metabolite quantitation in NIST plasma and pooled human plasma.

Introduction

Signaling lipids (SLs) are bioactive lipids that mediate a variety of signaling cascades in normal physiological functioning (e.g. pregnancy, exercise and appetite) and pathogenesis of diseases including inflammation, metabolic disorder and cancer [1]. The signaling lipid family encompasses different lipid moeities such as lysophospholipids, endocannabinoids, platelet activating factor (PAF), free fatty acids, oxylipins (including isoprostanes, prostaglandins and other hydroxy or epoxy oxidized lipids), sphingolipids and bile acids (**Figure 1**). Though chemically diverse, they are biologically intertwined via shared lipid precursors, regulating enzymes and interacting receptors resulting in functioning crosstalk. For example, the endocannabinoid system and bile acids regulate both energy and metabolic homeostasis [2-4], in interaction with gut microbiota and impacting intestinal inflammation [5-8]. The endocannabinoid and oxylipin classes are intertwined at both biosynthesis and biological action levels as was detailed in multiple reviews [9-11]. Notably, oxylipins represent typical inflammatory mediators and oxidative stress readouts mediated by enzymatic or non-enzymatic actions such as reactive oxygen species (ROS) [12,13]while endocannabinoids may modulate oxidative stress and lipid peroxidation through controlling mitochondrial-derived ROS or regulating cannabinoid receptors [14]. Sphingolipids are considered imperative in immune responses, cell survival and angiogenesis, cardiovascular system and neurodevelopment [15]. Their sphingoid backbone structure, and especially the phosphorylated form (sphingosine-1-phosphate), has been reported to directly modulate inflammatory responses [16,17] and to coordinate prostaglandin generation by affecting phospholipase A2 (PLA2) and cyclooxygenase 2 (COX-2) [18]. On the other hand, platelet-derived sphingosine-1-phosphate involves the maintenance of vascular integrity which can be induced by PAF with counteracting effect [19]. The signaling lipid network is further characterized by other reports describing the crosstalk between lysoglycerophospholipids sphingosine [20] and eicosanoids [21].

The essential roles of SLs discovered in pathophysiology has brought the momentum of advancing their metabolomic-based mass spectrometric profiling for better understanding of health and diseases. Methods covering relevant lipid classes have been developed and reported in the literature. A method targeting 37 oxylipins and 14 endocannabinoid was successfully developed and applied in tissues, cell, plasma and milk [22]. Lysophospholipid

profiling was advanced by several studies employing either qualitative [23,24] or quantitative [25,26] methods. Analytical approaches screening sphingosine-1-phosphate were described in several reports [27-29]. Bile acids were quantitated in the biofluid of mouse or human serum plasma and urine [30,31]. More recently, an ultra-high performance liquid chromatography–tandem mass spectrometry (UHPLC-MS/MS) method was developed with various signaling lipid classes quantified covering oxylipins, endocannabinoids, fatty acids, bile acids and steroids [32]. Despite of the plethora of available assays for signaling lipid profiling, there is no reported comprehensive method yet integrating all signaling lipid classes as illustrated in **Figure 1**.

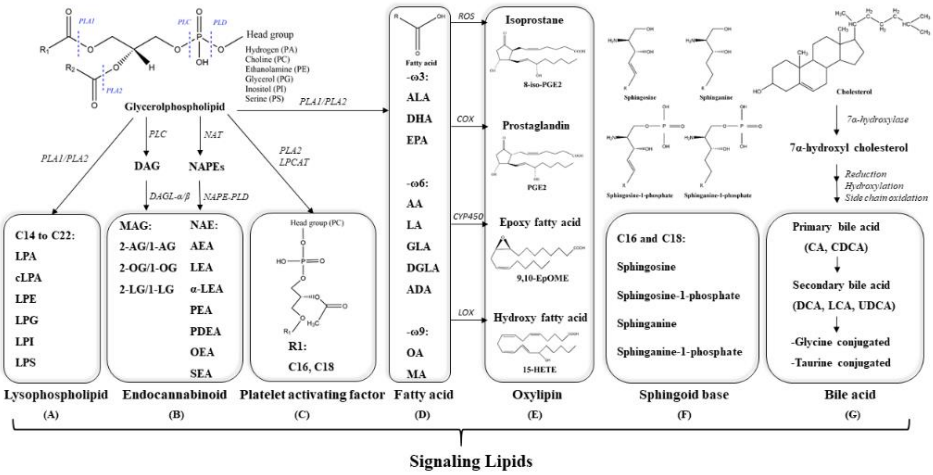

Figure 1. Simplified illustration of signaling lipid classes of lysophospholipid (A), endocannabinoid (B), platelet activating factor (C), fatty acid (D), oxylipin (E), sphingoid base (F) and bile acid (G).

Previously in our group we developed a targeted UHPLC-MS/MS metabolomics method enabling the measurement of 17 isoprostanes, 11 isomeric prostaglandin mediators, 3 nitro-fatty acids, 4 sphingoid mediators, 16 lysophospholipids (LPAs) and 6 cyclic LPAs (cLPAs) species [33]. This methodology was used as the starting point for an extended method aiming for including a broader range of signaling lipid molecules including additional oxylipins [34], endocannabinoids [35] as well as fatty acids and bile acids. In this study, we developed a

combined and comprehensive targeted UHPLC-MS/MS approach for signaling lipid profiling in human plasma after a simple and fast liquid-liquid extraction (LLE). The platform enables analyses of 261 metabolites covering oxylipins and their free fatty acid precursors, lysophospholipids, sphingoid bases, PAF, endocannabinoids and bile acids. The metabolites covered in this methodology can present readouts for the metabolic mediators underlying pathophysiological conditions pertaining to inflammation, oxidative stress and immune-dysfunction, and provide insights into the effect of the gut microbiome (on concentrations of gut metabolites or inducted metabolites in blood) as well as hormonal and metabolic control. The developed method shows good sensitivity and repeatability for metabolomics analysis of an extensive list of lipid based signaling molecules and provides a holistic biochemical picture orchestrated by the signaling lipid family.

Materials and Methods

Chemicals and Reagents

Ultra-performance liquid chromatography grade acetonitrile (ACN), methanol (MeOH), isopropyl alcohol (IPA) and MilliQ water were purchased from Biosolve (Valkenswaard, Netherlands). 1-Butanol (BuOH) was acquired from Boom (Meppel, Netherlands). Methyl tert-butyl ether (MTBE), acetic acid (100%, LC-MS grade), ammonium hydroxide, butylated hydroxytoluene (BHT), ethylenediaminetetraacetic acid (EDTA) and ammonium formate were from SigmaAldrich (Zwijndrecht, Netherlands). Citric acid monohydrate and disodium hydrogen phosphate were obtained from Merck (Darmstadt, Germany). Standards and deuterated standards for the isoprostanes, prostanoids and NO2-FAs were purchased from Cayman Chemicals (Ann Arbor, MI, USA). LPA and sphingoid base standards and uneven fatty acid length internal standards (ISTDs) were purchased from Avanti Polar Lipids (Alabaster, AL, USA).

Preparation of standards, ISTDs and calibrant solutions

Standard stock solutions were made in 12 mixes with MeOH containing BHT (0.4 mg/mL) and a calibration stock solution “C12” was prepared by mixing each standard stock solution. For target compounds, calibrant solutions were prepared with 11 different concentrations

(C1 to C11, 2 times dilution from level to level from C12 stock) and were used for the calibration lines. Calibrant solutions of standards were used for investigating linearity and sensitivity of target analyte which will be described in the following section. The volume of each calibrant solution used to prepare calibration samples was 10 µL.

ISTD stock solutions were made in 4 stock mixes with MeOH containing BHT (0.4 mg/mL) and the final ISTD mix was prepared by mixing 4 separate ISTD stock solutions. The volume of final ISTD mix used was 5 µL. Calibrant solutions of ISTDs were also prepared. Calibration stock solution "I9" was made by mixing each ISTD stock and calibrant solutions were prepared by diluting "I9" to 8 different concentrations (I1-I8, 2 times dilution from level to level). Calibrant solutions of ISTDs were used for investigating linearity and sensitivity of deuterated analyte which be described in the following section. The volume of each calibrant solution used to prepare calibration samples was 10 µL.

Biological samples of pooled human plasma, NIST SRM 1950

Pooled human plasma anti-coagulated with EDTA was purchased from Sanquin Blood Bank (Leiden, the Netherlands) and was used for method validation. Metabolite quantitation was performed along with method validation using both NIST SRM 1950 plasma and pooled human plasma to have a comparative overview of metabolite levels in two types of plasma samples. Technical replicates (n=9 in total) of NIST SRM 1950 and were aliquoted and measured with validation samples (3 samples per day). Commercially pooled human plasma samples were measured with five technical replicates per day and in total 15 aliquots.

Sample preparation protocols

An aliquot of 50 µL plasma or 50 µL water surrogate was used for liquid-liquid extraction of SLs. The extraction method was optimized based on a previously validated method [33]. After thawing on ice, 5 µL antioxidant (0.2mg/mL BHT and 0.2 mg/mL EDTA) solution and 5 µL ISTD solution were added to samples followed by brief vortexing. The samples were acidified with 50 µL of 0.2 M citric acid and 0.4 M disodium hydrogen phosphate buffer (pH 4.5). LLE was accomplished by the addition of 400 µL of the BuOH: MTBE (1:1 v: v) extraction solution followed by mixing for 4 min. All samples were centrifuged for 10 min at 4 °C and at 15800 rcf, after which 320 µL of the upper organic phase was collected and transferred to a clean 1.5 mL tube for drying *in SpeedVac (Thermo Fisher,*

USA). 50 µL of ice-cold injection solution (70% MeOH/30% ACN) was added to the dried residue to reconstitute the samples after which the samples were vortexed and centrifuged for 10 min at 4 °C and at 15800 rcf. The supernatants were transferred to injection vials with insert for LC-MS/MS analyses.

LC-MS/MS conditions

- High-pH run

Samples were analyzed by a LCMS-8060 system (Shimadzu,Japan) with a Kinetex® Core-Shell EVO 100 Å C18 Column (50 x 2.1 mm, 1.7 µm) maintained at 40 °C. The two-pump LC system consisted of mobile phase A (95 % H2O and 5 % Acetonitrile with 2 mM NH4HCO2 and 0.1 % NH3) and mobile phase B (95 % Acetonitrile with 5 % H2O with 2 mM NH4HCO2 and 0.1 % NH3) with pH ranges between 8.5 and 10.3. The injection volume was 5 µL. Chromatographic separation was achieved using a flow rate of 0.6 mL/min during a 11 min gradient which started at 1% mobile phase B followed by gradual increase of mobile phase B to 100% at 7.7 min. The condition of 100% mobile phase B was kept until 8.45 min and then dropped to 1% for reequilibration until 11 min.

The MS system used was a Shimadzu LCMS-8060 triple-quadrupole mass spectrometer with an electrospray ionization source. The electrospray ionization source parameters were set as follows: interface temperature 300 °C, desolvation line temperature 250 °C, heat block temperature 400 °C, nebulizing gas flow rate 3 L/min, heating gas flow rate 10 L/min and drying gas flow rate 10 L/min. Multiple reaction monitoring (MRM) with polarity switch scanning mode was applied for measurement of analytes and respective ISTDs. The detailed list of MRM transitions and retention time of each analyte with assigned ISTD group can be found in **Table S1**.

- Low-pH run

Samples were analyzed using a LCMS system of Shimadzu LC-30AD hyphenated to a SCIEX Triple-Quad 7500 system (USA) with a Waters Acquity® BEH C18 column (50 mm × 2.1 mm, 1.7 µm) maintained at 40 °C. The three-pump LC system consisted of mobile phase A (H_2O with 0.1 % acetic acid), mobile phase B (90 % ACN/10 % MeOH with 0.1 % acetic acid) and mobile phase C (IPA with 0.1 % acetic acid) with pH ranges between 3.2

and 3.5. The injection volume was 5 µL stacked with 10 µL of mobile phase A in the needle to increase column loadability. Chromatographic separation was achieved using a flow rate of 0.7 mL/min during a 16 min gradient which started at 20 % mobile phase B and 1% mobile phase C. The mobile phase B progressed from 20 % to 85 % between 0.75 min and 14 min while the mobile phase C ascended from 1 % to 15 % between 11 min to 14 min after which conditions were kept for 0.3 min and then the column was reequilibrated at initial conditions until 16 min.

The MS system of SCIEX Triple-Quad 7500 mass spectrometer used an electrospray ionization source with parameters: interface temperature 600 °C, curtain gas 45 psi, CAD gas 9, gas 1 and gas2 both 65 psi. Multiple reaction monitoring (MRM) with polarity switch scanning mode was applied for measurement of analytes and respective ISTDs. The detailed list of MRM transitions and retention time of each analyte with assigned ISTD group can be found in **Table S2**.

Method validation

Method performance was characterized by validation parameters including linearity (R^2), limit of detection (LOD), limit of quantification (LOQ), precision (intra-day and inter-day), extraction recovery and matrix effect.

- Linearity and sensitivity

Linearity was evaluated for both target analytes and deuterated compounds on three consecutive days. Calibration curves were determined for each target analyte using the ratio of analyte peak area to the corresponding ISTD peak area against spiked concentration. For deuterated compounds, calibration curves were determined for each ISTD using the ratio of ISTD peak area to the corresponding endogenous compound peak area against spiked concentration.

Limit of detection (LOD) and limit of quantification (LOQ) were calculated for both target compounds and ISTD compounds from obtained calibration curves following the equation

of LOD = 3.3 × Sa/b, LOQ = 10 × Sa/b, where Sa is the standard deviation of the y-intercept, b is the slope of the calibration curve [36].

-Intra-day and inter-day precision

Intraday precision and inter-day precision were investigated at low (C3), medium (C5,C7) and high (C9) levels. Intraday precision was determined by calculating the RSD of replicate (n=5) measurements of spiked samples within the same day while inter-day precision was evaluated at each level over 3 days.

-Extraction recovery and matrix effect

For all ISTDs, extraction recovery from both plasma and water as well as matrix effect were investigated with replicate samples (n=5) at three different levels (low, medium, high). To calculate recoveries, the ISTDs were spiked to the sample either before LLE or after LLE. The ratio of peak area from spiked-before sample to peak are from spiked-after samples was determined as recovery of each ISTD. To calculate matrix effect, the ISTDs were spiked to either the matrix or an academic blank solution. The matrix effect was determined by comparing the ISTD peak area in spiked blank and ISTD peak area in spiked plasma.

Data analyses

Raw data from high pH measurement and low pH measurement were firstly pre-processed by peak identification, integration and quantification using Shimadzu LabSolutions software package (version 5.65) and SCIEX OS-Q software (version 2.1.6) respectively. Relative intensity of each metabolite was acquired using the ratio of metabolite peak area to the peak area of respective deuterated ISTD.

Results and Discussion

Method development

Due to the diverse chemical nature of the signaling lipids, the development of a generic analytical method encompassing many classes of lipid molecules is challenging regarding several aspects: a) diversity of physicochemical properties of the metabolites; b) large

dynamic range of the metabolite concentrations; c) structurally similar isomeric species; d) difficulties in handling sample collection and sample storage to avoid artifacts. Therefore, during method development, care was taken to optimize sample handling, compound extraction and internal standard correction to compensate for recovery and matrix effect, and to optimize the chromatography to resolve isomers and minimize interference from coeluting compounds.

Firstly, we optimized the sample cleanup method and achieved simultaneous extraction of all SLs by using a fast liquid-liquid extraction (LLE). The endogenous concentrations of covered SLs present a significant wide range and this steered our extraction strategy, prioritizing analyte classes which require the highest possible recovery due to their low concentration and/or signal with MS. For example, the physiological level of the free fatty acids could be in the high micromolar range [37]. Bile acids and their conjugates could be present from low nanomolar level (GLCA, THDCA) to high nanomolar level (CDCA, DCA, GCA, GDCA, GUDCA) or even micromolar level (GCDCA) [38], while isoprostanes, prostanoids and endocannabinoids are only present at low nanomolar concentrations in human blood [39-41]. As both LLE and solid-phase extraction (SPE) have been applied previously for SLs extraction [33,34,42], we compared LLE and SPE. Though SPE had the advantage of cleaner extraction and higher recoveries of specific compound classes, one-step LLE presented overall better extraction with good repeatability. Furthermore, we optimized the LLE protocol by comparing different extraction solvents including Bligh & Dyer method, BuOH : EtOAc (v:v, 1:1) and BuOH: MTBE (v:v,1:1). The results demonstrated the best extraction performance with BuOH: MTBE (v:v,1:1), which was therefore selected as our final extraction protocol. In addition, with comparable analytical outcomes, a faster extraction achieved with the LLE protocol can reduce the possibility of compound degradation and oxidation which is important for introducing the least artifacts possible.

Secondly, we found the best chromatographic separation could be achieved by using two sample injections into two complimentary separations with different stationary phases and different gradients. We tailored a high pH run and a low pH run for the classes of SLs as detailed in [33]. As a result, the high pH separation method was developed for the measurement of lysophospholipids classes (LPA, LPE, LPG, LPI and LPS), free fatty acids,

sphingoid bases (phosphate form) and platelet activating factors (PAF). The optimized chromatography, with a fast 11-min gradient, enables good separation between lysophospholipid classes with different carbon chain lengths and double bounds. The Low pH separation method was developed for the measurement of oxylipins, sphingoid bases (non-phosphate form), endocannabinoids, bile acids and nitro free fatty acids. As we wanted to separate isomeric pairs (isoprostane and prostaglandin compounds) and various subclasses of oxylipins, our optimized chromatographic gradient was 16 mins. with oxylipin classes well separated across the entire gradient (**Figure 2**). Of note, some compound classes such as free fatty acids, bile acids and endocannabinoids can be detected well in both the high pH and low pH methods. For these, the optimal condition was selected based on peak intensity, peak shape and separation performance.

Thirdly, we optimized the choice of ISTD for each target compound. In general, stable isotopically labeled ISTDs have always been the most logical choice due to their almost identical physicochemical properties compared to target analytes [43]. In our study, deuterium-labeled ISTDs were used. For those targets where deuterated ISTDs are not commercially available, structural analogues or deuterated ISTDs from the same subfamily were chosen to correct for the target analyte which has been demonstrated in previous reports [44-46]. For example, one lysophosphatidyl lipid species in each subclass (LPA, LPC, LPE, LPG, LPS, and LPI) with an uneven chain length (C17:1) was used as internal standard for the analytes within the same lipid subclass. Oxylipins without available isotopically labeled standards were assigned to another deuterated ISTD from the same subclass with a similar retention time. Detailed information of targets with assigned ISTD is presented in supplementary **Table S1** and **Table S2**.

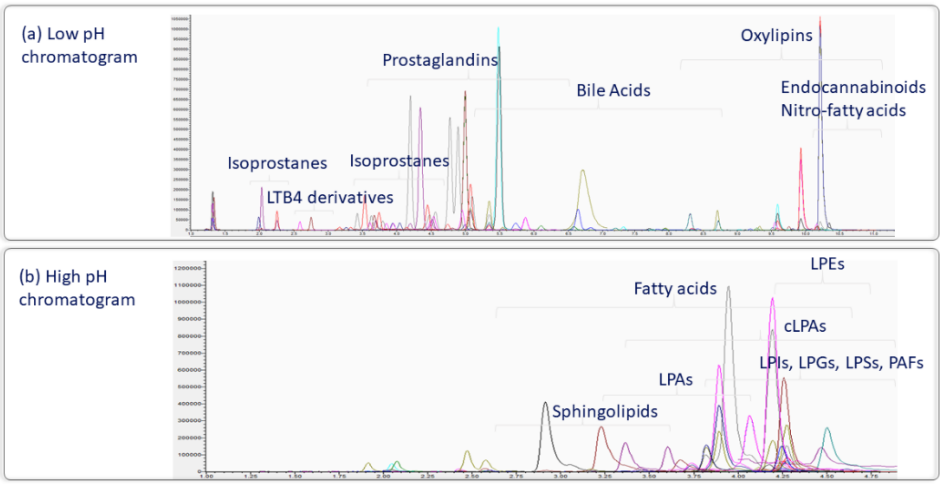

Figure 2. UHPLC-MS/MS chromatograms for (a) high pH run (b) low pH run.

Method Validation

The method performance was characterized by showing the robustness, sensitivity and reproducibility in profiling targeted compounds. In total, 261 target compounds were included in the method of which 187 target compounds had commercially available standards for reporting LOD, LOQ, linearity and precision and an additional 74 target compounds as structural analogues were screened with known ion masses. A total of 58 ISTDs were used for estimation of extraction recovery and matrix effect as well as LOD and LOQ. Results of extraction recovery and matrix effect are summarized in **Figure 3** (result of recovery from plasma extraction), supplemental **Figure S1** (result of recovery from water extraction), **Figure 4** (result of matrix effect from plasma extraction). Calculated LOD and LOQ and linearity are presented in **Table 1** (ISTDs) and **Table S3** (target compounds). Intra-day and inter-day precision results are shown in **Table 2**.

-Extraction recovery and matrix effect

Recoveries of 58 investigated ISTDs were calculated from plasma extraction and water extraction. The results are presented in **Figure 3** (recoveries from plasma extraction) and

Figure S1 (recoveries from water extraction). Overall, extraction recoveries are metabolite class dependent: in plasma at medium concentration levels, sphingoids 85%-99%, (nitro-) fatty acids 61%-67%, lysophospholipids 70%-104%, PAF 59%, oxylipins (isoprostane and prostanoid) > 80% except for d4-6-keto-PGF1a which was poorly recovered from plasma extraction, oxylipins (epoxy, hydroxy and keto acids) 74%-91% except for d11-8,9-EpETrE, bile acids 75%-91% and endocannabinoids 62%-70% except for d8-NADA with 47% recovery.

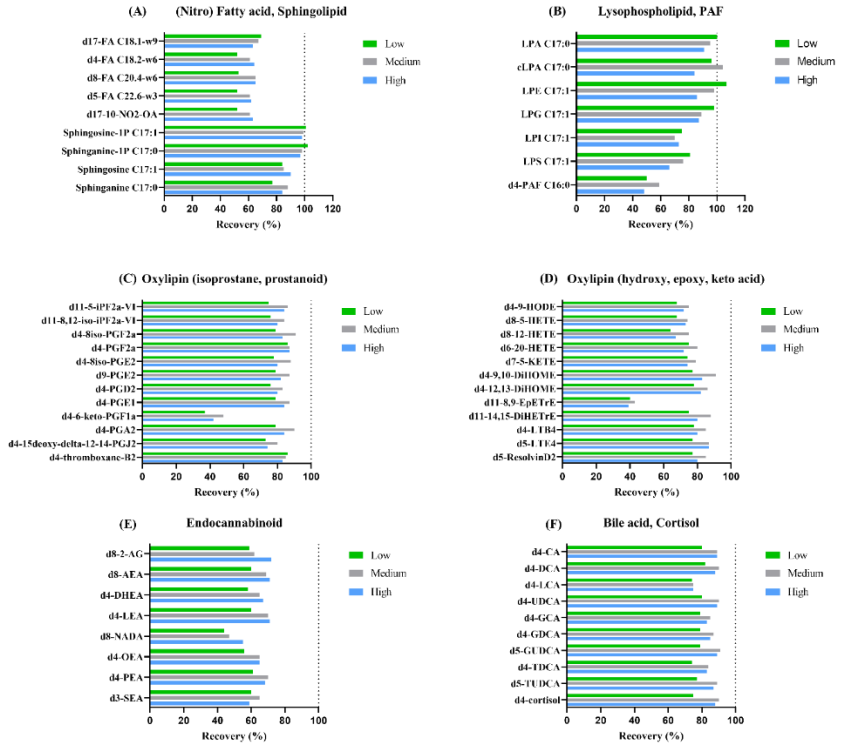

Figure 3. Recoveries of internal standards from plasma extraction at low, medium and high concentration level respectively shown by compound class (A) (nitro)-fatty acid, sphingolipid (B) lysophospholipid, PAF (C) Oxylipin (isoprostane, prostanoid) (D) Oxylipin (hydroxy, epoxy, keto acid) (E) Endocannabinoid (F) bile acid, cortisol.

Recoveries from water extractions showed differential patterns for some compound classes: free fatty acids were better extracted from water (73%-84% at medium level) while

sphingoids (68%-79% at medium level) and lysophospholipids (51%-72% at medium level) presented poorer recoveries. On three separate days, recovery experiments were repeated and the results showed recovery variability in plasma less than 15% for 56 ISTDs which demonstrated the repeatability of the LLE protocol.

The matrix effects were observed differentially across subclasses of signaling lipids of which some were ion suppressed while some were ion enhanced. (**Figure 4**). Analytes eluting at the end of the gradient showed higher levels of matrix effect and these late eluters included endocannabinoids (**Figure 4E**) and free fatty acids (**Figure 4A**). This could be attributed to co-eluting apolar lipids extracted by the chosen LLE method. This may also explain the higher variations of precision for endocannabinoids and fatty acids. Oxylipins (**Figure 4C, Figure 4D**) were slightly affected by matrix except that greater suppression was observed for four oxylipin ISTDs: d4-9-HODE (82%, 86%, 75% at low, medium, high level), d8-5-HETE (64%,61%,57% at low, medium, high level), d8-12-HETE (50%, 51%, 47% at low, medium, high level) and d11-8,9-EpETrE (53%, 66%, 58% at low, medium, high level). Sphingolipids (**Figure 4A**) and lysophospholipids (**Figure 4B**) experienced both ion-suppression and ion-enhancement dependent on compound species. Specifically, the non-phosphate form of sphingolipids had ion enhancement at low concentration levels (128%-154%) while the phosphate form of sphingolipids barely had matrix effect or subtle ion suppression (73%-102%). Slight suppression was shown in lysophospholipids of LPI C17:1 (91%, 80%, 80% at low, medium, high level) and LPS C17:1 (77%, 74%, 87% at low, medium, high level) and the rest presented enhanced matrix effect. Internal standard of d4-PAF C16:0 was mildly suppressed with 55%, 61% and 72% at low, medium, high level respectively. Bile acids (**Figure 4F**) were hardly affected by matrix effect at all investigated levels.

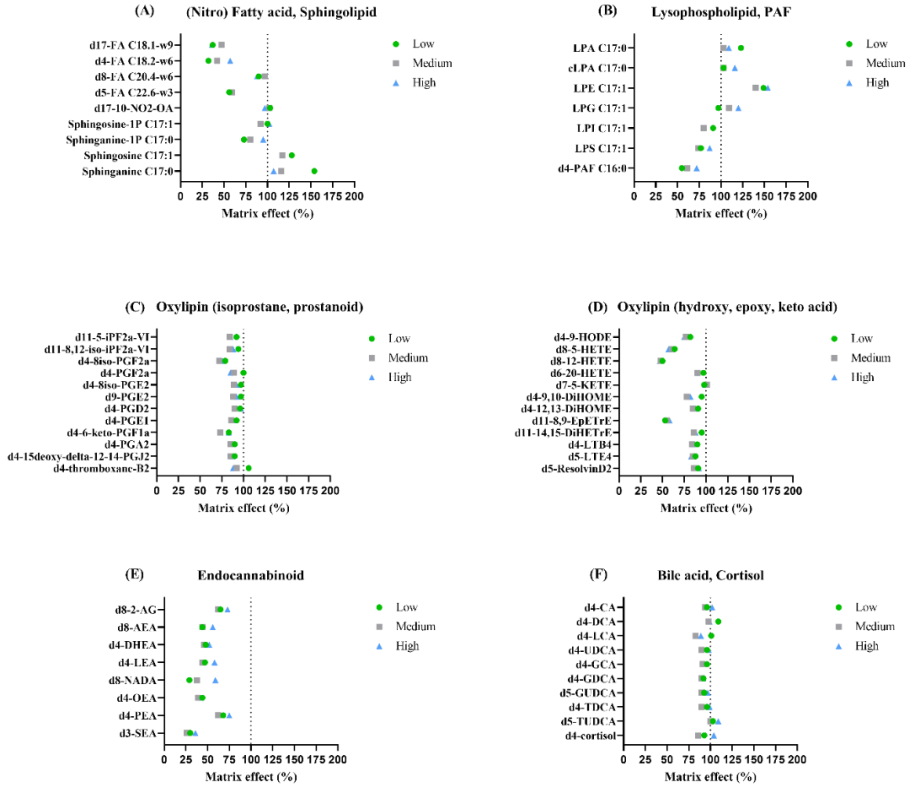

Figure 4. Matrix effect of internal standards from plasma extraction at low, medium and high concentration level respectively shown by compound class (A) (nitro)-fatty acid, sphingolipid (B) lysophospholipid, PAF (C) Oxylipin (isoprostane, prostanoid) (D) Oxylipin (hydroxy, epoxy, keto acid) (E) Endocannabinoid (F) bile acid, cortisol.

-Linearity and sensitivity

Among the 187 investigated targets with standards, most showed very good linearity in plasma with R^2>0.99 for 163 targets and R^2 between 0.98 and 0.99 for 24 targets (**Table S3**). Corresponding deuterated compounds (in total 58 ISTDs) presented good linearity in plasma with R^2 > 0.99 for 51 ISTDs and R^2>0.98 for 7 ISTDs (**Table 1**). Comparing LODs and LOQs calculated by target metabolite and by ISTD compound respectively, the overall result is comparable. For metabolites with high endogenous presence in plasma, plasma LODs and LOQs could be significantly higher than that calculated from academic solutions.

For instance, plasma LODs of lysophospholipid ISTDs ranged from 0.1-2.5 nM while plasma LODs of endogenous lysophospholipids ranged from 6-161 nM dependent on specific subclass. Oxylipin classes which had low endogenous levels in plasma had similar values comparing target metabolite and deuterated compound. Compared with another analytical method which combines oxylipins, endocannabinoids, bile acids and steroids [32], our method presents remarkable advantages for oxylipin profiling with a broader coverage of oxylipin targets including an additional list of isoprostanes and prostaglandins and higher sensitivity. The median LOD values for isoprostanes and prostanoids (1-series, 2-series and 3-series collectively) were 0.038 nM and 0.083 nM for academic and plasma determination respectively and were 3.5 time lower than published LOD value (0.29 nM) [32]. For PGE1 and PGF3α, plasma LOD value in our method were 13 and 10 times lower respectively compared to published data [32]. For specialized lipid mediators including leukotrienes, resolvins and protectins, detection sensitivity was increased by 8-41 times [32].

For endocannabinoid profiling, sensitivity enhancement of our method is highlighted by AEA, DEA, DHEA, PEA, DGLEA and SEA. Of note, background interferences originating from solvents used was seen for PEA, PDEA and SEA and only samples where the background level was less than 40% of the measured signal were included for LOD LOQ calculation and further analyses. For monoacylglycerols (MAGs), due to isomerization between 1- and 2-acylchain, the sum of two acylchains was used to present MAG level (1-AG & 2-AG; 2-OG & 2-OG; 1-LG & 2-LG) in each sample.

Table 1. Plasma LOD, LOQ and linearity of deuterated signaling lipids

ISTD identifier (Fatty acid)	**LOD (nM)**	**LOQ (nM)**	**R^2**
d17-FA C18:1	1.822	5.466	0.9855
d4-FA C18:2	0.556	1.668	0.9913
d8-FA C20:4	0.867	2.601	0.9960
d5-FA C22:6	0.455	1.366	0.9980
d17-10-O_2-OA	1.165	3.496	0.9928
ISTD identifier (Sphingoid base)	**LOD (nM)**	**LOQ (nM)**	**R^2**
Sphingosine1P C17:1	0.084	0.252	0.9948
Sphinganine1P C17:0	0.283	0.849	0.9950
Sphingosine C17:1	0.593	1.778	0.9981

Sphinganine C17:0	0.362	1.085	0.9883
ISTD identifier (Lysophospholipid, PAF)	**LOD (nM)**	**LOQ (nM)**	**R^2**
LPA C17:0	0.935	2.806	0.9945
cLPA C17:0	2.516	7.547	0.9982
LPE C17:1	0.145	0.435	0.9920
LPG C17:1	0.340	1.020	0.9974
LPI C17:1	1.687	5.060	0.9970
LPS C17:1	0.529	1.587	0.9918
d4-PAF C16:0	0.319	0.957	0.9976
ISTD identifier (Oxylipin)	**LOD (nM)**	**LOQ (nM)**	**R^2**
d11-5-iPF2α -VI	0.071	0.213	0.9986
d11-8,12-iso-iPF2α -VI	0.009	0.026	0.9996
d4-8iso-PGF2α	0.225	0.675	0.9867
d4-PGF2α	0.465	1.395	0.9964
d4-8iso-PGE2	0.089	0.268	0.9928
d9-PGE2	0.020	0.060	0.9997
d4-PGD2	0.076	0.228	0.9998
d4-PGE1	0.023	0.068	0.9988
d4-6-keto-PGF1α	0.327	0.980	0.9883
d4-PGA2	0.006	0.018	0.9966
d4-15deoxy-delta-12-14-PGJ2	0.166	0.497	0.9980
d4-thromboxane-B2	0.464	1.392	0.9967
d4-9-HODE	0.058	0. C174	0.9970
d8-5-HETE	0.660	1.981	0.9971
d8-12-HETE	0.094	0.282	0.9969
d6-20-HETE	0.382	1.146	0.9994
d7-5-KETE	0.967	2.902	0.9993
d4-9,10-DiHOME	0.2 C17	0.652	0.9979
d4-12,13-DiHOME	0.044	0.131	0.9990
d11-8,9-EpETrE	0.234	0.701	0.9897
d11-14,15-DiHETrE	0.006	0.0 C17	0.9948
d4-LTB4	0.044	0.133	0.9979
d5-LTE4	0.031	0.093	0.9991
d5-ResolvinD2	0.007	0.022	0.9974
ISTD identifier (Endocannabinoid)	**LOD (nM)**	**LOQ (nM)**	**R^2**
d8-2-AG	1.532	4.596	0.9909
d8-AEA	0.026	0.077	0.9909

d4-DHEA	0. 171	0.514	0.9961
d4-LEA	0.180	0.539	0.9972
d8-NADA	7.091	21.273	0.9961
d4-OEA	0.444	1.333	0.9949
d4-PEA	2.709	8.127	0.9886
d3-SEA	0.242	0.726	0.9896
ISTD identifier (Bile acid and cortisol)	**LOD (nM)**	**LOQ (nM)**	**R^2**
d4-CA	0.233	0.700	0.9981
d4-DCA	12.467	37.402	0.9965
d4-LCA	1.187	3.560	0.9904
d4-UDCA	1.079	3.236	0.9990
d4-GCA	0.144	0.433	0.9974
d4-GDCA	0.345	1.036	0.9984
d5-GUDCA	0.482	1.446	0.9995
d4-TDCA	0.425	1.276	0.9988
d5-TUDCA	20.020	60.061	0.9901
d4-cortisol	27.348	82.045	0.9957

- Intra-day and inter-day precision

Summarized results of intra-day and inter-day precision by metabolite class is presented in **Table 2**. For all metabolites, intra-day variation is lower than 15% except for few oxylipin compounds and endocannabinoid compounds with intra-day variation 15%-20% (only low concentration level). For inter-batch effects, metabolite classes of sphingoid base, lysophospholipid, PAF and bile acid showed inter-day variability lower than 15% at all investigated levels. Most oxylipin compounds presented good inter-day precision. At low, medium and high level respectively, 89.6%, 95.2% and 95.2% oxylipins had inter-day variance <15%; 7.2%, 0.8% and 0.8% with variance between 15% and 20% and the rest higher than 20%. Oxylipins of E-series leukotrienes, thromboxane B3, HpETEs (12-,15-), 13-HpODE, 13-KODE and 15-KETE accounted for high variabilities of >20%.

Endocannabinoids and fatty acids showed relatively higher variabilities (RSD between 20%-30%) compared to other subclasses probably due to matrix effect which may influence more significantly on hydrophobic analytes.

Table 2. Summarized intra-day and inter-day precision of signaling lipid by class

Metabolite class	Intra-day precision (%)			Inter-day precision (%)		
	low	medium	high	low	medium	high
Sphingoid base	1.7-8.5	1.0-3.8	1.4-5.8	4.0-9.7	3.9-9.1	4.2-11.2
Lysophospholipid and PAF	4.2-8.3	2.7-8.2	1.8-6.4	6.5-14.1	4.7-11.8	7.0-10.8
Free fatty acid	2.7-12.3	3.2-11.3	2.3-7.4	5.6-25.2	3.0-24.5	4.9-27.9
Oxylipin (isoprostane, prostanoid)	1.2-15.5	0.9-5.5	1.0-12.5	2.4-34.0	2.2-28.3	3.6-17.5
Oxylipin (epoxy, hydroxy)	0.9-14.6	0.9-10.5	1.0-9.2	3.0-19.0	3.1-22.9	4.3-22.7
Endocannabinoid	3.6-17.1	1.8-13.2	2.1-14.3	5.1-24.4	4.4-27.0	4.9-29.1
Bile acid	1.9-10.3	1.2-10.8	1.8-6.4	4.6-14.1	3.6-10.2	3.2-10.4

Metabolite quantitation in NIST SRM 1950 and pooled human plasma

Metabolites were quantified in both NIST SRM 1950 plasma and pooled human plasma using calibration lines made the same day. In total, 187 target analytes with commercially available standards were included for quantitation and the full results were reported in **Table S4**. In NIST SRM 1950 plasma and pooled human plasma respectively, 109 metabolites and 145 metabolites were successfully quantified. Targets not detected in plasma or with signal to noise ratio lower than 3 were reported as NA. Fatty acid concentrations were not provided since relatively high variance among technical replicates were observed. To obtain an overview of our quantitation results, comparative analysis was performed by correlating metabolite concentrations in NIST plasma measured by our method with available reference concentrations reported by NIST (for oxylipins and bile acids) [47] or by the group of John W. Newman (first reports of endocannabinoids) [32]. **Figure 5** demonstrates good correlation between our data and published data for all metabolites (**Figure 5A**) as well as in data subsets grouped by lipid class (**Figure 5B , 5C, 5D**).

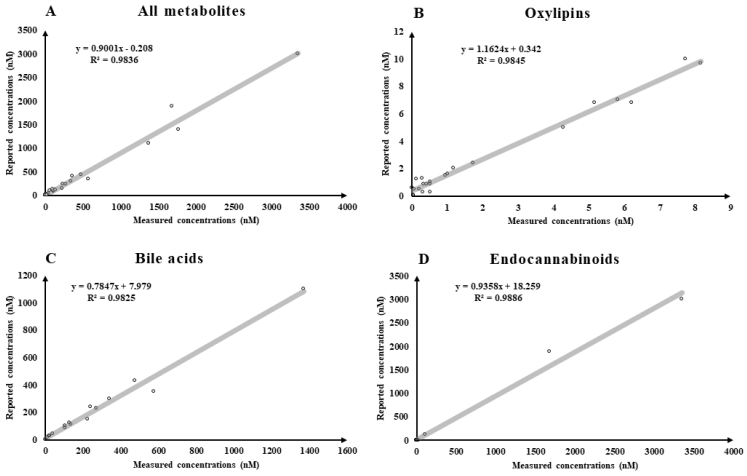

Figure 5. Correlation plots of metabolite concentrations in NIST SRM 1950: measured concentrations vs reported concentrations by including (A) all metabolites (B) oxylipins only (C) bile acids only (D) endocannabinoids only. For endocannabinoids, measured concentration values in this study were correlated with reported concentrations by the group of John W. Newman. For other metabolite subclasses, metabolites with coefficient of dispersion (COD) values lower than 40% according to NIST reports were included for correlation.

Nevertheless, discrepancies between quantitation results when comparing our data with published data were seen, and these metabolites with high variance were mostly oxylipin compounds (**Figure 5B**). For instance, oxylipins of HETEs, HEPEs and HDoHEs quantified in our dataset were much lower than the values reported by NIST [47]. PGD2 in NIST SRM 1950 was 0.463 nM in our measurement which was higher than reported 0.17 nM [48] but comparable with another publication reporting 0.473 nM [32]. Of note, very high coefficient of dispersion (COD) values of these compounds were observed, which suggest the reference concentration was summarized from "inconsistent" measurements across labs [47]. In consideration of the susceptibility of oxylipins to temperature, storage time and sample treatment procedures [48-50], we must not neglect artifacts introduced which can increase data variability. Therefore interlaboratory comparisons should be taken with caution for these metabolites.

In this study, we provided for the first time concentrations of 37 signaling lipids in NIST SRM 1950 plasma covering 23 oxylipins (5 isoprostanes, 4 prostanoids, 3 leukotrienes, 2 lipoxins, 1 protectin and 8 other oxylipins), 2 nitro-free fatty acids, 7 lysophospholipids, 1 bile acid and 4 endocannabinoids (**Table 3**). Specifically, lower LODs of isoprostanes, prostanoids and nitro-free fatty acids (~0.1nM or lower) enabled us to quantify nitro-free fatty acids and a broader list of isoprostanes in plasma which were previously not reported by other studies.

Table 3. New reports of concentrations of 37 signaling lipids in NIST SRM 1950 and in pooled human plasma

Compound	Concentration in pooled human plasma (nM)	Concentration in NIST SRM 1950 (nM)
Lysophospholipid		
LPA C16:0	3302	521
LPA C18:0	370	140
LPA C18:1	339	95
LPA C20:4	779	257
cLPA C18:1	446	55
LPG C18:1	54	57
LPS C18:1	46	3.716
Nitro fatty acid		
NO_2-LA	0.625	0.603
NO_2-OA	0.127	1.433
Oxylipin (Isoprostane)-DGLA derived		
8-iso-PGA1	0.942	0.375
Oxylipin (Isoprostane)-AA derived		
5-iPF2α-VI	4.833	0.446
8,12-iso-iPF2α-VI	28	4.680
8-iso-PGA2	0.223	0.030
8-iso-15keto-PGF2β	0.672	0.375
Oxylipin (Prostanoid)-DGLA derived		
PGE1	1.489	0.032
6-keto-PGF1α	0.671	0.636
Oxylipin (Prostanoid)-AA derived		
11β-PGF2α	1.119	1.527
PGA2	0.593	0.038
Oxylipin (Leukotriene)-AA derived		
20-carboxy-LTB4	0.061	0.039
6trans-LTB4	22	1.381
LTE4	NA	0.079
Oxylipin (Lipoxin)-AA derived		
5S,6R-lipoxinA4	6.837	1.162
5S,14R-lipoxinB4	9.495	2.005

Oxylipin (Protectin)-DHA derived		
10,17-DiHDoHE	2.737	0.007
Oxylipin (others)-LA derived		
9,10,13-TriHOME	3.608	1.561
13-KODE	1.527	1.365
Oxylipin (others)-ALA derived		
9-HOTrE	0.545	0.044
Oxylipin (others)-EPA derived		
14,15-DiHETE	NA	0.438
Oxylipin (others)-DHA derived		
19,20-EpDPE	1.867	0.167
7-HDoHE	3.284	0.966
13-HDoHE	15	0.074
16-HDoHE	5.705	0.081
Bile acid		
THDCA	0.339	0.227
Endocannabinoid		
POEA	0.449	0.752
PDEA [a]	0.356	0.380
PEA [a]	4.823	9.713
SEA [a]	4.858	9.128

Measured concentrations of each metabolite are mean values calculated from technical replicates and with S/N higher than 3 if the value is lower than LOD.

NA: Metabolite without detected peak or peak intensity too low for accurate quantitation.

[a] Metabolite with caution, relatively higher background in blank sample.

Conclusion and Perspective

In this study, we successfully developed and characterized a comprehensive UHPLC-MS/MS method targeting a wide range of classes of signaling lipids. Even though quite a few analytical methods have been reported before for individual classes, our platform is unique in its coverage of a broad range of signaling lipids including lysophospholipids, sphingoid bases, platelet activating factors, fatty acids, oxylipins, endocannabinoids and bile acids, and several resolvins. Having optimized sample extraction, LC gradient, MS parameters, and injection solution, our method has been shown to be fast, sensitive, reproducible and robust. Compared to the published method targeting similar metabolites which was built on SCIEX 6500, our validated method on SCIEX 7500 presented a significant sensitivity increase especially for prostaglandins, isoprostanes and specialized lipid mediators. With promising applicability, this validated method is expected to be a powerful platform providing profiling of signaling lipids which are essential biomarkers for oxidative stress and dynamics of immune responses such as indicating the processes of pro-inflammatory, anti-inflammatory and pro-resolutionary cascades. We performed metabolite quantitation in NIST SRM 1950 plasma and pooled human plasma and provided metabolite concentrations in both types of plasma which will be informative for researchers who work on lipidomics fields. The characterization of signaling lipids from biological samples will offer innovative insights into related biomedical mechanisms as well as novel diagnostic and prognostic targets for clinical treatment.

Acknowledgement

This research was part of the Netherlands X-omics Initiative and partially funded by NWO, project 184.034.019.Wei Yang would like to acknowledge the Chinese Scholarship Council (CSC, No. 201607060017) for the financial support.

References

1. Wymann MP, Schneiter R. Lipid signalling in disease. Nat Rev Mol Cell Biol. 2008;9(2):162-176.

2. Di Marzo V, Matias I. Endocannabinoid control of food intake and energy balance. Nat Neurosci. 2005;8(5):585-589.

3. Osei-Hyiaman D, Harvey-White J, Batkai S, Kunos G. The role of the endocannabinoid system in the control of energy homeostasis. Int J Obes (Lond). 2006;30 Suppl 1:S33-38.

4. Lefort C, Cani PD. The Liver under the Spotlight: Bile Acids and Oxysterols as Pivotal Actors Controlling Metabolism. Cells. 2021;10(2).

5. Shapiro H, Kolodziejczyk AA, Halstuch D, Elinav E. Bile acids in glucose metabolism in health and disease. J Exp Med. 2018;215(2):383-396.

6. Cani PD, Plovier H, Van Hul M, et al. Endocannabinoids--at the crossroads between the gut microbiota and host metabolism. Nat Rev Endocrinol. 2016;12(3):133-143.

7. de Vos WM, Tilg H, Van Hul M, Cani PD. Gut microbiome and health: mechanistic insights. Gut. 2022;71(5):1020-1032.

8. Jia W, Xie G, Jia W. Bile acid-microbiota crosstalk in gastrointestinal inflammation and carcinogenesis. Nat Rev Gastroenterol Hepatol. 2018;15(2):111-128.

9. Rouzer CA, Marnett LJ. Endocannabinoid oxygenation by cyclooxygenases, lipoxygenases, and cytochromes P450: cross-talk between the eicosanoid and endocannabinoid signaling pathways. Chem Rev. 2011;111(10):5899-5921.

10. Burstein SH. Eicosanoid mediation of cannabinoid actions. Bioorg Med Chem. 2019;27(13):2718-2728.

11. Buisseret B, Alhouayek M, Guillemot-Legris O, Muccioli GG. Endocannabinoid and Prostanoid Crosstalk in Pain. Trends Mol Med. 2019;25(10):882-896.

12. Dennis EA, Norris PC. Eicosanoid storm in infection and inflammation. Nat Rev Immunol. 2015;15(8):511-523.

13. Rund KM, Heylmann D, Seiwert N, et al. Formation of trans-epoxy fatty acids correlates with formation of isoprostanes and could serve as biomarker of oxidative stress. Prostaglandins Other Lipid Mediat. 2019;144:106334.

14. Gallelli CA, Calcagnini S, Romano A, et al. Modulation of the Oxidative Stress and Lipid Peroxidation by Endocannabinoids and Their Lipid Analogues. Antioxidants (Basel). 2018;7(7).

15. Hannun YA, Obeid LM. Sphingolipids and their metabolism in physiology and disease. Nat Rev Mol Cell Biol. 2018;19(3):175-191.

16. Gomez-Munoz A, Presa N, Gomez-Larrauri A, Rivera IG, Trueba M, Ordonez M. Control of inflammatory responses by ceramide, sphingosine 1-phosphate and ceramide 1-phosphate. Prog Lipid Res. 2016;61:51-62.

17. Maceyka M, Spiegel S. Sphingolipid metabolites in inflammatory disease. Nature. 2014;510(7503):58-67.

18. Pettus BJ, Kitatani K, Chalfant CE, et al. The coordination of prostaglandin E2 production by sphingosine-1-phosphate and ceramide-1-phosphate. Mol Pharmacol. 2005;68(2):330-335.

19. Vito CD, Hadi LA, Navone SE, et al. Platelet-derived sphingosine-1-phosphate and inflammation: from basic mechanisms to clinical implications. Platelets. 2016;27(5):393-401.

20. Shea BS, Tager AM. Role of the lysophospholipid mediators lysophosphatidic acid and sphingosine 1-phosphate in lung fibrosis. Proc Am Thorac Soc. 2012;9(3):102-110.

21. Artru F, McPhail MJW, Triantafyllou E, Trovato FM. Lipids in Liver Failure Syndromes: A Focus on Eicosanoids, Specialized Pro-Resolving Lipid Mediators and Lysophospholipids. Front Immunol. 2022;13:867261.

22. Gouveia-Figueira S, Nording ML. Validation of a tandem mass spectrometry method using combined extraction of 37 oxylipins and 14 endocannabinoid-related compounds including prostamides from biological matrices. Prostaglandins Other Lipid Mediat. 2015;121(Pt A):110-121.

23. Lisa M, Cifkova E, Holcapek M. Lipidomic profiling of biological tissues using off-line two-dimensional high-performance liquid chromatography-mass spectrometry. J Chromatogr A. 2011;1218(31):5146-5156.

24. Lee JY, Min HK, Moon MH. Simultaneous profiling of lysophospholipids and phospholipids from human plasma by nanoflow liquid chromatography-tandem mass spectrometry. Anal Bioanal Chem. 2011;400(9):2953-2961.

25. Koistinen KM, Suoniemi M, Simolin H, Ekroos K. Quantitative lysophospholipidomics in human plasma and skin by LC-MS/MS. Anal Bioanal Chem. 2015;407(17):5091-5099.

26. Okudaira M, Inoue A, Shuto A, et al. Separation and quantification of 2-acyl-1-lysophospholipids and 1-acyl-2-lysophospholipids in biological samples by LC-MS/MS. J Lipid Res. 2014;55(10):2178-2192.

27. Butter JJ, Koopmans RP, Michel MC. A rapid and validated HPLC method to quantify sphingosine 1-phosphate in human plasma using solid-phase extraction followed by derivatization with fluorescence detection. J Chromatogr B Analyt Technol Biomed Life Sci. 2005;824(1-2):65-70.

28. Scherer M, Schmitz G, Liebisch G. High-throughput analysis of sphingosine 1-phosphate, sphinganine 1-phosphate, and lysophosphatidic acid in plasma samples by liquid chromatography-tandem mass spectrometry. Clin Chem. 2009;55(6):1218-1222.

29. Egom EE, Fitzgerald R, Canning R, Pharithi RB, Murphy C, Maher V. Determination of Sphingosine-1-Phosphate in Human Plasma Using Liquid Chromatography Coupled with Q-Tof Mass Spectrometry. Int J Mol Sci. 2017;18(8).

30. Alnouti Y, Csanaky IL, Klaassen CD. Quantitative-profiling of bile acids and their conjugates in mouse liver, bile, plasma, and urine using LC-MS/MS. J Chromatogr B Analyt Technol Biomed Life Sci. 2008;873(2):209-217.

31. Gomez C, Stucheli S, Kratschmar DV, Bouitbir J, Odermatt A. Development and Validation of a Highly Sensitive LC-MS/MS Method for the Analysis of Bile Acids in Serum, Plasma, and Liver Tissue Samples. Metabolites. 2020;10(7).

32. Pedersen TL, Gray IJ, Newman JW. Plasma and serum oxylipin, endocannabinoid, bile acid, steroid, fatty acid and nonsteroidal anti-inflammatory drug quantification in a 96-well plate format. Anal Chim Acta. 2021;1143:189-200.

33. Schoeman JC, Harms AC, van Weeghel M, Berger R, Vreeken RJ, Hankemeier T. Development and application of a UHPLC-MS/MS metabolomics based comprehensive systemic and tissue-specific screening method for inflammatory, oxidative and nitrosative stress. Anal Bioanal Chem. 2018;410(10):2551-2568.

34. Strassburg K, Huijbrechts AM, Kortekaas KA, et al. Quantitative profiling of oxylipins through comprehensive LC-MS/MS analysis: application in cardiac surgery. Anal Bioanal Chem. 2012;404(5):1413-1426.

35. Kantae V, Ogino S, Noga M, et al. Quantitative profiling of endocannabinoids and related N-acylethanolamines in human CSF using nano LC-MS/MS. J Lipid Res. 2017;58(3):615-624.

36. Shrivastava A, Gupta VB. Methods for the determination of limit of detection and limit of quantitation of the analytical methods. Chron. Young Sci. 2011;2(1):21-25.

37. Christinat N, Morin-Rivron D, Masoodi M. High-Throughput Quantitative Lipidomics Analysis of Nonesterified Fatty Acids in Plasma by LC-MS. Methods Mol Biol. 2017;1619:183-191.

38. Han J, Liu Y, Wang R, Yang J, Ling V, Borchers CH. Metabolic profiling of bile acids in human and mouse blood by LC-MS/MS in combination with phospholipid-depletion solid-phase extraction. Anal Chem. 2015;87(2):1127-1136.

39. Sanchez-Moreno C, Cano MP, de Ancos B, et al. Mediterranean vegetable soup consumption increases plasma vitamin C and decreases F2-isoprostanes, prostaglandin E2 and monocyte chemotactic protein-1 in healthy humans. J Nutr Biochem. 2006;17(3):183-189.

40. Zilio AM, Zielinsky P, Vian I, et al. Polyphenol supplementation inhibits physiological increase of prostaglandin E2 during reproductive period - A randomized clinical trial. Prostaglandins Leukot Essent Fatty Acids. 2018;136:77-83.

41. Gachet MS, Rhyn P, Bosch OG, Quednow BB, Gertsch J. A quantitiative LC-MS/MS method for the measurement of arachidonic acid, prostanoids, endocannabinoids, N-acylethanolamines and steroids in human plasma. J Chromatogr B Analyt Technol Biomed Life Sci. 2015;976-977:6-18.

42. Ostermann AI, Willenberg I, Schebb NH. Comparison of sample preparation methods for the quantitative analysis of eicosanoids and other oxylipins in plasma by means of LC-MS/MS. Anal Bioanal Chem. 2015;407(5):1403-1414.

43. Stokvis E, Rosing H, Beijnen JH. Stable isotopically labeled internal standards in quantitative bioanalysis using liquid chromatography/mass spectrometry: necessity or not? Rapid Commun Mass Spectrom. 2005;19(3):401-407.

44. Valbuena H, Shipkova M, Kliesch SM, Muller S, Wieland E. Comparing the effect of isotopically labeled or structural analog internal standards on the performance of a LC-MS/MS method to determine ciclosporin A, everolimus, sirolimus and tacrolimus in whole blood. Clin Chem Lab Med. 2016;54(3):437-446.

45. Godfrey AR, Jones L, Davies M, Townsend R. Miltefosine: a novel internal standard approach to lysophospholipid quantitation using LC-MS/MS. Anal Bioanal Chem. 2017;409(11):2791-2800.

46. Bodnar-Broniarczyk M, Pawinski T, Kunicki PK. Isotope-labeled versus analog internal standard in LC-MS/MS method for tacrolimus determination in human whole blood samples - A compensation of matrix effects. J Chromatogr B Analyt Technol Biomed Life Sci. 2019;1104:220-227.

47. Bowden J, Ulmer CZ, Jones CM, Heckert NA. Lipid concentrations in standard reference material (SRM) 1950: Results from an Interlaboratory Comparison Exercise for Lipidomics. 2017.

48. Ramsden CE, Yuan ZX, Horowitz MS, et al. Temperature and time-dependent effects of delayed blood processing on oxylipin concentrations in human plasma. Prostaglandins Leukot Essent Fatty Acids. 2019;150:31-37.

49. Koch E, Mainka M, Dalle C, et al. Stability of oxylipins during plasma generation and long-term storage. Talanta. 2020;217:121074.

50. Rund KM, Nolte F, Doricic J, et al. Clinical blood sampling for oxylipin analysis - effect of storage and pneumatic tube transport of blood on free and total oxylipin profile in human plasma and serum. Analyst. 2020;145(6):2378-2388.

Supplementary files

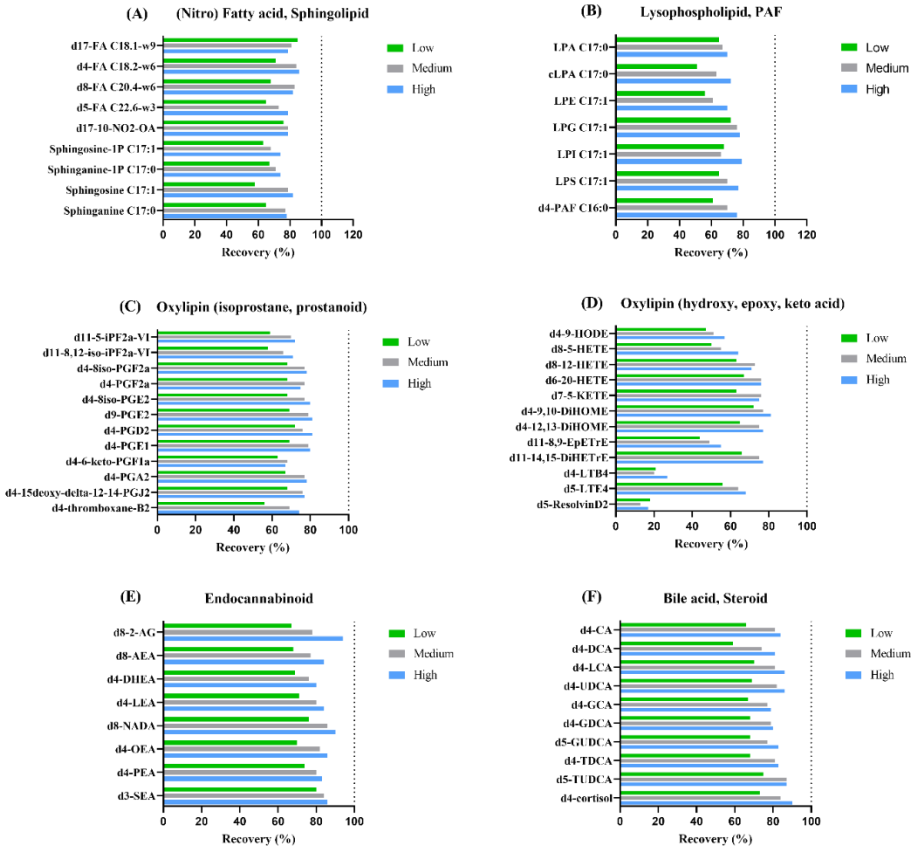

Figure S1: Recoveries of internal standards from water extraction at low, medium and high concentration level respectively shown by compound class (A) (nitro)-fatty acid, sphingolipid (B) lysophospholipid, PAF (C) Oxylipin (isoprostane, prostanoid) (D) Oxylipin (hydroxy, epoxy, keto acid) (E) Endocannabinoid (F) bile acid, cortisol.

Table S1: High pH run target list and corresponding ISTDs with detailed LCMS information

Metabolite Name	Type	ISTD Group	Precursor (Da)	Product (Da)	RT (min)	MS polarity
Sphingosine-1P C16:1	Target	Sphingosine-1P C17:1	350	79.05	2.90	Neg
Sphinganine-1P C18:0	Target	Sphinganine-1P C17:0	380	79.05	4.00	Neg
Sphingosine-1P C18:1	Target	Sphingosine-1P C17:1	378.1	79.05	3.74	Neg
Sphingosine-1P C18:2	Target	Sphingosine-1P C17:1	376.1	79.05	3.22	Neg
Sphinganine-1P C17:0	ISTD		366	79.05	3.48	Neg
Sphingosine-1P C17:1	ISTD		364	79	3.18	Neg
LPA C14:0	Target	LPA C17:0	381.2	153.05	3.24	Neg
LPA C16:0	Target	LPA C17:0	409	153.05	3.99	Neg
LPA C16:1	Target	LPA C17:0	407.2	153.05	3.51	Neg
LPA C17:0	ISTD		423.2	153.05	4.16	Neg
LPA C18:0	Target	LPA C17:0	437.3	153.05	4.51	Neg
LPA C18:1	Target	LPA C17:0	435.2	153.05	4.07	Neg
LPA C18:2	Target	LPA C17:0	433.2	153.05	3.66	Neg
LPA C20:3	Target	LPA C17:0	459.2	153.05	4.12	Neg
LPA C20:4	Target	LPA C17:0	457	153.05	3.89	Neg
LPA C20:5	Target	LPA C17:0	455.2	153.05	3.54	Neg
LPA C22:4	Target	LPA C17:0	485.2	153.05	4.38	Neg
LPA C22:5	Target	LPA C17:0	483.2	153.05	4.12	Neg
LPA C22:6	Target	LPA C17:0	481.2	153.05	3.80	Neg
cLPA C14:0	Target	cLPA C17:0	363.1	227	5.28	Neg
cLPA C16:0	Target	cLPA C17:0	390.9	255	5.33	Neg
cLPA C16:1	Target	cLPA C17:0	389.1	253	4.65	Neg
cLPA C17:0	ISTD		405.2	269.25	5.50	Neg
cLPA C18:0	Target	cLPA C17:0	419.1	283	5.89	Neg
cLPA C18:1	Target	cLPA C17:0	417.2	281	5.37	Neg
cLPA C18:2	Target	cLPA C17:0	415.1	279	4.96	Neg
cLPA C20:4	Target	cLPA C17:0	439.1	303	4.99	Neg
cLPA C20:5	Target	cLPA C17:0	437.1	301	4.59	Neg
LPE C14:0	Target	LPE C17:1	424.4	196.15	4.71	Neg
LPE C16:0	Target	LPE C17:1	452.4	196.15	5.50	Neg
LPE C16:1	Target	LPE C17:1	450.4	196.15	4.98	Neg
LPE C17:1	ISTD		464.4	267.35	5.28	Neg
LPE C18:0	Target	LPE C17:1	480.4	196.25	6.30	Neg
LPE C18:1	Target	LPE C17:1	478.4	196.25	5.74	Neg
LPE C18:2	Target	LPE C17:1	476.4	196.25	5.25	Neg

LPE C18:3	Target	LPE C17:1	474.4	196.25	4.94	Neg
LPE C20:3	Target	LPE C17:1	502.4	196.15	5.60	Neg
LPE C20:4	Target	LPE C17:1	500.4	196.15	5.31	Neg
LPE C20:5	Target	LPE C17:1	498.4	196.15	4.89	Neg
LPE C22:4	Target	LPE C17:1	528.4	196.15	5.91	Neg
LPE C22:5	Target	LPE C17:1	526.4	196.15	5.54	Neg
LPE C22:6	Target	LPE C17:1	524.4	196.15	5.34	Neg
LPG C14:0	Target	LPG C17:1	455.1	227.3	4.14	Neg
LPG C16:0	Target	LPG C17:1	483.1	255.3	4.85	Neg
LPG C16:1	Target	LPG C17:1	481.1	253.3	4.35	Neg
LPG C17:1	ISTD		495.4	267.3	4.68	Neg
LPG C18:0	Target	LPG C17:1	511.1	283.3	5.52	Neg
LPG C18:1	Target	LPG C17:1	509.1	281.3	5.04	Neg
LPG C18:2	Target	LPG C17:1	507.1	279.3	4.62	Neg
LPG C18:3	Target	LPG C17:1	505.1	277.3	4.30	Neg
LPG C20:3	Target	LPG C17:1	533.1	305.3	5.03	Neg
LPG C20:4	Target	LPG C17:1	531.1	303.3	4.79	Neg
LPG C20:5	Target	LPG C17:1	529.1	301.3	4.30	Neg
LPG C22:4	Target	LPG C17:1	559.1	331.3	5.21	Neg
LPG C22:6	Target	LPG C17:1	555.1	327.3	4.73	Neg
LPS C16:0	Target	LPS C17:1	496.1	153.05	4.48	Neg
LPS C17:1	ISTD		508.4	153.2	4.09	Neg
LPS C18:0	Target	LPS C17:1	524.1	153.05	4.91	Neg
LPS C18:1	Target	LPS C17:1	522.4	153.1	4.44	Neg
LPS C18:2	Target	LPS C17:1	520.1	153.05	4.06	Neg
LPS C20:4	Target	LPS C17:1	544.1	153.05	4.10	Neg
LPS C22:4	Target	LPS C17:1	572.1	153.05	4.61	Neg
LPS C22:6	Target	LPS C17:1	568.1	153.05	4.15	Neg
LPI C14:0	Target	LPI C17:1	543.2	227.2	4.02	Neg
LPI C16:0	Target	LPI C17:1	571.1	255.25	4.70	Neg
LPI C16:1	Target	LPI C17:1	569.1	253.25	4.26	Neg
LPI C17:1	ISTD		583.4	267.3	4.48	Neg
LPI C18:0	Target	LPI C17:1	599.1	283.25	5.37	Neg
LPI C18:1	Target	LPI C17:1	597.1	281.25	4.83	Neg
LPI C18:2	Target	LPI C17:1	595.1	153.05	4.54	Neg
LPI C20:4	Target	LPI C17:1	619.1	303.25	4.59	Neg
LPI C22:4	Target	LPI C17:1	647.2	331.2	5.10	Neg
LPI C22:6	Target	LPI C17:1	643.2	327.2	4.62	Neg

d4-PAF C16:0	ISTD		572.2	59	6.65	Neg
PAF C16:0	Target	d4-PAF C16:0	524.2	125.1	6.64	Pos
PAF C16:0_adduct	Target	d4-PAF C16:0	568.3	59.1	6.60	Neg
PAF C18:2_adduct	Target	d4-PAF C16:0	592.3	59.1	6.49	Neg
CUDA	Reference		339.3	214.25	2.45	Neg

Table S2: Low pH run target list and corresponding ISTDs with detailed LCMS information

Metabolite Name	Type	ISTD Group	Precursor (Da)	Product (Da)	RT (min)	MS polarity
Cortisol	Target	d4-cortisol	363	121	1.88	Pos
d4-cortisol	ISTD		367	121	1.87	Pos
α-LEA	Target	d4-LEA	322	62	11.92	Pos
POEA	Target	d4-OEA	298	62	12.42	Pos
PDEA	Target	d8-AEA	286	62	12.76	Pos
d4-LEA	ISTD		328.3	66.2	12.86	Pos
d4-DHEA	ISTD		376.3	66.2	12.9	Pos
LEA	Target	d4-LEA	324	62	12.86	Pos
AEA	Target	d8-AEA	348	62	12.9	Pos
d8-AEA	ISTD		356.3	62.2	12.87	Pos
DHEA	Target	d4-DHEA	372	62	12.87	Pos
d8-2-AG	ISTD		387.3	294.2	13.15	Pos
1-AG & 2-AG	Target	d8-2-AG	379.21	287	13.25	Pos
d4-PEA	ISTD		304.3	62.2	13.21	Pos
1-LG & 2-LG	Target	d4-PEA	355	263	13.3	Pos
PEA	Target	d4-PEA	300	62	13.23	Pos
DGLEA	Target	d4-OEA	350	62	13.16	Pos
2-AGE	Target	d4-OEA	365	273	13.35	Pos
DEA	Target	d3-SEA	376	62	13.34	Pos
1-OG & 2-OG	Target	d4-OEA	357	265	13.61	Pos
d3-SEA	ISTD		331.3	62.2	13.67	Pos
SEA	Target	d3-SEA	328	62	13.69	Pos
NADA	Target	d8-NADA	440	137	13.2	Pos
d8-NADA	ISTD		448.4	137	13.18	Pos
OEA	Target	d4-OEA	326	62	13.3	Pos
d4-OEA	ISTD		330.3	66.2	13.33	Pos
EPEA	Target	d4-LEA	346	62	12.08	Pos
ETAEA	Target	d4-OEA	350	289	13.28	Pos

Sphingosine C18:1	Target	Sphingosine C17:1	300.1	282.2	12.62	Pos
Sphinganine C18:0	Target	Sphinganine C17:0	302.5	284.15	13.09	Pos
Sphingosine C17:1	ISTD		286	238.3	11.21	Pos
Sphinganine C17:0	ISTD		288.1	59.8	11.95	Pos
20-hydroxy-PGF2α	Target	d4-PGF2α	369.2	325.2	1.27	Neg
20-hydroxy-PGE2	Target	d9-PGE2	367.2	287.2	1.28	Neg
2,3dinor-8iso-PGF2α	Target	d4-8iso-PGF2α	325.1	237.2	1.91	Neg
20-carboxy-LTB4	Target	d4-LTB4	365.2	347.2	2.56	Neg
2,3dinor-11b-PGF2α	Target	d4-PGF2α	325	145.2	2.13	Neg
20-hydroxy-LTB4	Target	d4-LTB4	351.2	195.2	2.62	Neg
iPF2α-IV	Target	d11-5-iPF2α-VI	353.3	127.1	3.28	Neg
8-iso-15R-PGF2α	Target	d4-8iso-PGF2α	353.1	193.1	3.34	Neg
8-iso-PGF2α	Target	d4-8iso-PGF2α	353.1	193.1	3.57	Neg
11β-PGF2α	Target	d4-PGF2α	353.1	193.1	3.74	Neg
PGF2α	Target	d4-PGF2α	353.1	193.1	4.53	Neg
PGE3	Target	d4-PGE2	349.2	269.2	3.54	Neg
PGD3	Target	d4-PGD2	349.2	269.2	3.62	Neg
d4-8-iso-PGF2α	ISTD		357.3	197.15	3.53	Neg
d4-PGF2α	ISTD		357.3	197.15	4.48	Neg
d4-thromboxane-B2	ISTD		373.5	173.3	3.62	Neg
8-iso-PGE2	Target	d4-8iso-PGE2	351.1	271.15	4.49	Neg
PGE2	Target	d9-PGE2	351.1	271.15	4.74	Neg
11β-PGE2	Target	d9-PGE2	351.1	271.15	4.9	Neg
PGD2	Target	d4-PGD2	351.1	271.15	5.12	Neg
thromboxane-B2	Target	d4-thromboxane-B2	369.2	169.1	3.64	Neg
d11-5-iPF2α-VI	ISTD		364.2	115.05	3.9	Neg
d11-8,12-iso-iPF2α-VI	ISTD		364.21	115.05	5.82	Neg
5-iPF2α-VI	Target	d11-5-iPF2α-VI	353.2	115.05	4	Neg
8,12-iso-iPF2α-VI	Target	d11-8,12-iso-iPF2α-VI	353.21	115.05	5.95	Neg
9,12,13-TriHOME	Target	d4-PGF2α	329.2	211.1	4.12	Neg
9,10,13-TriHOME	Target	d4-PGF2α	329.2	171.1	4.29	Neg
d4-8iso-PGE2	ISTD		355.3	275.25	4.47	Neg
d4-PGE2	ISTD		355.3	275.25	4.71	Neg
d4-PGD2	ISTD		355.3	275.25	5.09	Neg
d9-PGE2	ISTD		360.3	280.25	4.7	Neg
8iso-13,14dihydro-15keto-PGF2α	Target	d4-8iso-PGF2α	353.3	183.1	4.5	Neg
13,14dihydro-15keto-PGF2α	Target	d4-PGF2α	353.31	183.1	5.88	Neg

d5-GUDCA	ISTD		453.3	74.1	4.79	Neg
GUDCA	Target	d5-GUDCA	448.2	74	4.92	Neg
13,14dihydro-PGF2α	Target	d4-PGF2α	355.2	311.3	5.3	Neg
GCA	Target	d4-GCA	464.2	74.1	5.38	Neg
d4-GCA	ISTD		468.3	74.05	5.37	Neg
13,14dihydro-15keto-PGE2	Target	d9-PGE2	351.2	175.1	5.72	Neg
13,14dihydro-15keto-PGD2	Target	d4-PGD2	351.21	175.1	6.66	Neg
5S,6R-lipoxinA4	Target	d4-LTB4	351.2	115.2	6.12	Neg
5S,6S-lipoxinA4	Target	d4-LTB4	351.21	115.2	6.54	Neg
1a,1b-dihomo-PGF2α	Target	d4-PGF2α	381.1	337.45	7.3	Neg
d4-CA	ISTD		411.2	347.3	7.99	Neg
CA	Target	d4-CA	407.3	343.3	8	Neg
GCDCA	Target	d4-GDCA	448.21	74	8.23	Neg
GDCA	Target	d4-GDCA	448.22	74	8.66	Neg
bicyclo-PGE2	Target	d9-PGE2	333.2	113.15	8.3	Neg
12,13-DiHODE	Target	d4-12,13-DiHOME	311.2	293.15	8.33	Neg
CUDA	Target		339.3	214.25	9.25	Neg
d4-GDCA	ISTD		452.3	74.15	8.69	Neg
8,15-DiHETE	Target	d4-LTB4	335.2	235.1	8.64	Neg
10,17-DiHDoHE	Target	d4-LTB4	359.2	153.1	9.02	Neg
17,18-DiHETE	Target	d11-14,15-DiHETrE	335.2	247.1	8.83	Neg
14,15-DiHETE	Target	d11-14,15-DiHETrE	335.2	207.1	9.1	Neg
d4-LTB4	ISTD		339.5	197.1	9.17	Neg
d4-12,13-DiHOME	ISTD		317.2	185.1	9.26	Neg
12,13-DiHOME	Target	d4-12,13-DiHOME	313.2	183.1	9.3	Neg
d4-9,10-DiHOME	ISTD		317.2	203.1	9.49	Neg
9,10-DiHOME	Target	d4-9,10-DiHOME	313.2	201.05	9.52	Neg
d11-14,15-DiHETrE	ISTD		348.2	207.1	9.74	Neg
14,15-DiHETrE	Target	d11-14,15-DiHETrE	337.2	207.1	9.77	Neg
12-HHTrE	Target	d4-12,13-DiHOME	279.2	179.1	9.79	Neg
19,20-DiHDPA	Target	d11-14,15-DiHETrE	361.2	273.2	9.85	Neg
CDCA	Target	d4-DCA	391.2	373.25	10.19	Neg
11,12-DiHETrE	Target	d11-14,15-DiHETrE	337.2	167.3	10.05	Neg
d4-DCA	ISTD		395.3	349.1	10.14	Neg
DCA	Target	d4-DCA	391.2	345.25	10.15	Neg
9-HOTrE	Target	d4-9-HODE	293.2	171.2	10.23	Neg
8,9-DiHETrE	Target	d11-14,15-DiHETrE	337.2	127.2	10.28	Neg

GLCA	Target	d4-DCA	432.3	74.1	10.3	Neg
18-HEPE	Target	d8-12-HETE	317.2	299.2	10.32	Neg
15-HEPE	Target	d6-20-HETE	317.2	219.2	10.54	Neg
d6-20-HETE	ISTD		325.2	279.2	10.56	Neg
20-HETE	Target	d6-20-HETE	319.2	289.2	10.63	Neg
5,6-DiHETrE	Target	d11-14,15-DiHETrE	337.2	145.15	10.64	Neg
12-HEPE	Target	d8-12-HETE	317.2	179.1	10.73	Neg
9-HEPE	Target	d8-12-HETE	317.2	167.25	10.86	Neg
13-HODE	Target	d4-9-HODE	295.2	195.2	10.99	Neg
12,13-EpOME	Target	d4-12,13-DiHOME	295.21	195.2	12.32	Neg
5-HEPE	Target	d4-9-HODE	317.2	115.2	11.02	Neg
d4-9-HODE	ISTD		299.2	172.1	11.03	Neg
9-HODE	Target	d4-9-HODE	295.21	171.1	11.08	Neg
9,10-EpOME	Target	d4-9,10-DiHOME	295.22	171.1	12.47	Neg
17-HDoHE	Target	d8-12-HETE	343.2	281.2	11.49	Neg
13-HDoHE	Target	d8-12-HETE	343.2	281.2	11.58	Neg
7-HDoHE	Target	d8-12-HETE	343.2	281.2	11.99	Neg
4-HDoHE	Target	d8-12-HETE	343.2	281.2	12.52	Neg
19,20-EpDPE	Target	d11-14,15-DiHETrE	343.2	281.2	12.37	Neg
20-HDoHE	Target	d8-12-HETE	343.21	299.2	11.17	Neg
15-HETE	Target	d8-5-HETE	319.2	219.2	11.29	Neg
14,15-EpETrE	Target	d11-14,15-DiHETrE	319.21	219.2	12.46	Neg
16-HDoHE	Target	d8-12-HETE	343.2	233.2	11.41	Neg
16,17-EpDPE	Target	d11-14,15-DiHETrE	343.21	233.2	12.66	Neg
11-HETE	Target	d8-12-HETE	319.2	167.1	11.59	Neg
9-HETE	Target	d8-12-HETE	319.21	167.1	11.59	Neg
11,12-EpETrE	Target	d11-8,9-EpETrE	319.22	167.1	12.75	Neg
d8-12-HETE	ISTD		327.2	184.1	11.74	Neg
14-HDoHE	Target	d8-12-HETE	343.2	205.1	11.68	Neg
10-HDoHE	Target	d8-12-HETE	343.21	153.1	11.72	Neg
12-HETE	Target	d8-12-HETE	319.2	179.2	11.76	Neg
8-HETE	Target	d8-5-HETE	319.2	155.1	11.82	Neg
8,9-EpETrE	Target	d11-8,9-EpETrE	319.21	167.1	12.85	Neg
d11-8,9-EpETrE	ISTD		330.21	167.1	12.76	Neg
11-HDoHE	Target	d8-12-HETE	343.2	121.1	11.85	Neg
15-HETrE	Target	d8-5-HETE	321.2	221.1	12	Neg
8-HDoHE	Target	d8-12-HETE	343.2	189.1	12.09	Neg

d8-5-HETE	ISTD		327.1	116.15	12.14	Neg
5-HETE	Target	d8-5-HETE	319.2	115.15	12.22	Neg
8-HETrE	Target	d8-5-HETE	321.2	303.2	12.25	Neg
5-HETrE	Target	d8-5-HETE	321.21	303.2	12.98	Neg
NO_2-αLA	Target	d17-10-NO_2-OA	322.2	46.05	13	Neg
10-NO_2-LA	Target	d17-10-NO_2-OA	324.2	277.25	13.02	Neg
d17-10-NO_2-OA	ISTD		343.2	183.2	13.22	Neg
10-NO_2-OA;9-NO_2-OA	Target	d17-10-NO_2-OA	326.2	279.2	13.24	Neg
FA C16:0	Target	d17-FA C18:1-w9	255.2	237.2	13.7	Neg
FA C18:0	Target	d17-FA C18:1-w9	283.2	265.2	14	Neg
FA C18:1-w9	Target	d17-FA C18:1-w9	281.1	263.2	13.82	Neg
FA C18:2-w6	Target	d4-FA C18:2-w6	279.2	261.2	13.53	Neg
FA C18:3-w3	Target	d4-FA C18:2-w6	277	233	13.3	Neg
FA C18:3-w6	Target	d4-FA C18:2-w6	277	233	13.21	Neg
FA C20:3-w3	Target	d8-FA C20:4-w6	305.1	261	13.48	Neg
FA C20:3-w6	Target	d8-FA C20:4-w6	305.1	261	13.64	Neg
FA C20:3-w9	Target	d8-FA C20:4-w6	305.1	261	13.7	Neg
FA C20:4-w6	Target	d8-FA C20:4-w6	303	259	13.47	Neg
FA C20:5-w3	Target	d8-FA C20:4-w6	301.1	257.2	13.22	Neg
FA C22:4-w6	Target	d5-FA C22:6-w3	331.5	287.5	13.74	Neg
FA C22:5-w3	Target	d5-FA C22:6-w3	329.1	179	13.41	Neg
FA C22:5-w6	Target	d5-FA C22:6-w3	329.1	179	13.53	Neg
FA C22:6-w3	Target	d5-FA C22:6-w3	327.1	283.1	13.4	Neg
d17-FA C18:1-w9	ISTD		298.1	298.1	13.78	Neg
d4-FA C18:2-w6	ISTD		283.2	283.2	13.49	Neg
d4-FA C18:2-w6-2	ISTD		283.2	265.201	13.51	Neg
d8-FA C20:4-w6	ISTD		311.1	267.2	13.46	Neg
d5-FA C22:6-w3	ISTD		332.1	288.4	13.4	Neg
d5-TUDCA	ISTD		503.201	80	2.78	Neg
d4-TUDCA	ISTD		502.201	80	2.82	Neg
TUDCA	Target	d5-TUDCA	498.201	80	2.82	Neg
THDCA	Target	d5-TUDCA	498.201	80	3.02	Neg
d5-TDCA	ISTD		503.2	80	6.13	Neg
d4-TDCA	ISTD		502.2	80	6.13	Neg
TCDCA	Target	d5-TDCA	498.2	80	5.6	Neg
TDCA	Target	d5-TDCA	498.2	80	6.15	Neg
TCA	Target	d4-GCA	514.2	80	3.29	Neg

TLCA	Target	d4-CA	482.2	80	8.5	Neg
TLCA-3S	Target	d4-GCA	584	464.35	5.38	Neg
LCA-3S	Target	d4-DCA	455.2	97	10.28	Neg
d4-LCA	ISTD		379.3	379.3	12.19	Neg
LCA	Target	d4-LCA	375.3	375.3	12.22	Neg
d4-UDCA	ISTD		395.3	395.3	7.8	Neg
UDCA	Target	d4-UDCA	391.3	391.3	7.82	Neg
HDCA	Target	d4-CA	391.2	391.2	8.26	Neg
HCA	Target	d4-CA	407.3	407.3	7.06	Neg
6trans-LTB4	Target	d4-LTB4	335.2	195.1	8.98	Neg
LTB4	Target	d4-LTB4	335.2	195.1	9.21	Neg
LTB5	Target	d4-LTB4	333.2	195.1	7.88	Neg
14,15-LTE4	Target	d5-LTE4	438.2	333.2	7.93	Neg
LTE4	Target	d5-LTE4	438.2	333.2	8.84	Neg
11trans-LTE4	Target	d5-LTE4	438.2	333.2	9.15	Neg
d5-LTE4	ISTD		443.2	338.2	8.81	Neg
PGJ2	Target	d4-15deoxy-delta-12-14-PGJ2	333.2	233.1	7.56	Neg
15deoxy-delta-12,14-PGJ2	Target	d4-15deoxy-delta-12-14-PGJ2	315.1	271.1	10.7	Neg
d4-15deoxy-delta-12,14-PGJ2	ISTD		319.1	275.1	10.41	Neg
8iso-PGE1	Target	d4-PGE1	353.2	317.2	4.71	Neg
PGE1	Target	d4-PGE1	353.2	317.2	5.13	Neg
d4-PGE1	ISTD		357.2	321.2	5.11	Neg
PGF1α	Target	d4-PGF2α	355.2	311.1	4.64	Neg
PGK2	Target	d4-PGD2	349.2	205.1	5.11	Neg
8iso-PGF3α	Target	d4-8iso-PGF2α	351.2	193.2	2.53	Neg
PGF3α	Target	d4-PGF2α	351.2	193.2	3.24	Neg
8iso-PGA1	Target	d4-PGA2	335.2	273.2	7.25	Neg
PGA1	Target	d4-PGA2	335.2	273.2	7.75	Neg
8iso-PGA2	Target	d4-PGA2	333	271.3	7.14	Neg
PGA2	Target	d4-PGA2	333	271.3	7.27	Neg
d4-PGA2	ISTD		337	275.3	7.23	Neg
thromboxane-B1	Target	d4-thromboxane-B2	371.2	171.1	3.42	Neg
thromboxane-B3	Target	d4-thromboxane-B2	367.2	169.1	2.6	Neg
LipoxinA5	Target	d4-PGF2α	349.1	115	4.34	Neg
Maresin1	Target	d4-12,13-DiHOME	359.1	177	9.1	Neg
ResolvinD1	Target	d5-ResolvinD2	375.3	141	6.19	Neg
ResolvinD2	Target	d5-ResolvinD2	375.3	175	5.4	Neg

d5-ResolvinD2	ISTD		380.3	175	5.32	Neg
ResolvinD3	Target	d5-ResolvinD2	375.3	147	5	Neg
ResolvinD5	Target	d4-12,13-DiHOME	359.1	199.1	9.1	Neg
ResolvinE1	Target	d5-ResolvinD2	349.3	195	2.39	Neg
ResolvinE2	Target	d5-ResolvinD2	333.3	115.1	3	Neg
12-HpETE	Target	d8-5-HETE	335.2	273.2	12.35	Neg
15-HpETE	Target	d8-12-HETE	335.2	113.1	11.69	Neg
5-KETE	Target	d7-5-KETE	317.2	203.2	12.54	Neg
d7-5-KETE	ISTD		324.2	210.2	12.71	Neg
12-KETE	Target	d8-5-HETE	317.2	273.3	12.02	Neg
15-KETE	Target	d8-12-HETE	317.2	113.2	11.69	Neg
14,15-EpETE	Target	d8-12-HETE	317.2	207.1	11.62	Neg
17,18-EpETE	Target	d8-12-HETE	317.2	259.2	11.24	Neg
15keto-PGF2α	Target	d4-PGF2α	351.2	219.1	4.82	Neg
13,14dihydro-15keto-PGF1α	Target	d4-PGF2α	355.2	193.2	6.64	Neg
9-HpODE	Target	d4-9,10-DiHOME	311.2	185.2	9.37	Neg
13-HpODE	Target	d4-9-HODE	311.2	113.2	11.42	Neg
9-KODE	Target	d4-9-HODE	293.2	185.2	11.59	Neg
13-KODE	Target	d8-5-HETE	293.2	113.1	11.42	Neg
13-HOTE	Target	d4-9,10-DiHOME	293.2	171.2	9.7	Neg
5S,14R-lipoxinB4	Target	d5-ResolvinD2	351.2	221.2	5.04	Neg
6-keto-PGE1	Target	d4-6-keto-PGF1α	367.2	143.1	2.35	Neg
6-keto-PGF1α	Target	d4-6-keto-PGF1α	369.2	163.1	2.29	Neg
d4-6-keto-PGF1α	ISTD		373.2	167.1	2.29	Neg
delta17-6-keto-PGF1α	Target	d4-6-keto-PGF1α	367.2	163.1	1.65	Neg
15-keto-PGF1α	Target	d4-PGF2α	353.2	221.1	6.72	Neg
13,14dihydro-15keto-PGD1	Target	d4-PGF2α	353.2	209.1	7.3	Neg
15deoxy-12-14-PGD2	Target	d4-12,13-DiHOME	333.2	271.2	9.11	Neg
PGB2	Target	d4-PGF2α	333.2	235	7.43	Neg
8iso-15keto-PGE2	Target	d4-PGE2	349	113	5	Neg
8iso-15keto-PGF2β	Target	d4-PGF2α	351.1	315.15	3.76	Neg
8iso-15keto-PGF2α	Target	d4-PGF2α	351.1	315.15	3.9	Neg
PGA3	Target	d4-PGF2α	331	215	5.68	Neg
5,15-DiHETE	Target	d4-9,10-DiHOME	335.3	173.1	8.9	Neg

Table S3. LOD, LOQ (in water and in plasma respectively) and linearity of each metabolite

Compound	LOD (nM) Water	LOQ (nM) Water	LOD (nM) Plasma	LOQ (nM) Plasma	Linearity R^2 Plasma
Sphingoid base					
Sphinganine C18:0	0.677	2.032	1.538	4.615	0.9972
Sphingosine C18:1	0.526	1.578	2.211	6.632	0.9957
Sphinganine-1-phosphate C18:0	0.710	2.130	1.500	4.500	0.9942
Sphingosine-1-phosphate C18:1	2.220	6.660	10.000	30.000	0.9979
Lysophospholipid					
LPA C16:0	0.250	0.750	42.960	128.880	0.9946
LPA C18:0	0.660	1.980	30.890	92.670	0.9946
LPA C18:1	0.300	0.900	33.370	100.110	0.9978
LPA C20:4	0.580	1.740	26.840	80.520	0.9946
cLPA C18:1	7.770	23.310	49.430	148.290	0.9867
LPE C18:1	3.870	11.610	161.340	484.020	0.9877
LPG C18:1	0.050	0.150	18.970	56.910	0.9974
LPS C18:1	0.340	1.020	6.150	18.450	0.9821
LPI C20:4	1.180	3.540	28.650	85.950	0.9851
Platelet Activating Factor					
PAF C16:0	1.630	4.890	0.580	1.740	0.9989
Free fatty acid					
FA C18:1 w9 (OA)	1147	3441			0.9893
FA C18:2 w6 (LA)	1150	3450			0.9994
FA C18:3 w3 (ALA)	85	255			0.9971
FA C18:3 w6 (GLA)	126	378			0.9971
FA C20:3 w6 (DGLA)	89	267			0.9990
FA C20:3 w9 (MA)	11	33			0.9814
FA C20:4 w6 (AA)	42	126			0.9917
FA C20:5 w3 (EPA)	8.240	24.720			0.9941
FA C22:4 w6 (ADA)	4.060	12.180			0.9908
FA C22:6 w3 (DHA)	19	57			0.9907
Nitro fatty acid					
NO_2-LA	0.168	0.503	0.180	0.541	0.9969

NO_2-OA	0.220	0.660	0.113	0.339	0.9985
Oxylipin (Isoprostane)-DGLA derived					
8-iso-PGA1	0.038	0.113	0.053	0.159	0.9919
8-iso-PGE1	0.012	0.037	0.044	0.133	0.9973
Oxylipin (Isoprostane)-AA derived					
2,3dinor-8-iso-PGF2α	0.041	0.122	0.119	0.357	0.9973
8-iso-15R-PGF2α	0.025	0.075	0.091	0.274	0.9978
8-iso-PGF2α	0.013	0.039	0.190	0.571	0.9987
8-iso-PGE2	0.116	0.348	0.232	0.697	0.9939
5-iPF2α-VI	0.005	0.015	0.058	0.173	0.9986
8,12-iso-iPF2α-VI	0.252	0.757	0.404	1.211	0.9963
8-iso-13,14-dihydro-15keto-PGF2α	0.050	0.150	0.009	0.027	0.9971
8-iso-PGA2	0.063	0.188	0.043	0.129	0.9955
8-iso-15keto-PGE2	0.028	0.084	0.112	0.337	0.9910
8-iso-15keto-PGF2β	0.010	0.031	0.076	0.227	0.9983
8-iso-15keto-PGF2α	0.010	0.031	0.038	0.113	0.9991
Oxylipin (Isoprostane)-EPA derived					
8-iso-PGF3α	0.053	0.160	0.021	0.063	0.9950
Oxylipin (Prostanoid)-DGLA derived					
PGA1	0.054	0.162	0.034	0.102	0.9981
PGE1	0.052	0.156	0.044	0.131	0.9953
PGF1α	0.019	0.058	0.044	0.133	0.9911
13,14-dihydro-15keto-PGF1α	0.048	0.144	0.059	0.178	0.9984
6-keto-PGF1α	0.838	2.515	0.038	0.115	0.9942
13,14-dihydro-15keto-PGD1	0.038	0.115	0.045	0.135	0.9989
thromboxane-B1	0.043	0.129	0.015	0.046	0.9960
Oxylipin (Prostanoid)-AA derived					
20-hydroxy-PGF2α	0.061	0.183	0.038	0.114	0.9978
20-hydroxy-PGE2	0.025	0.074	0.315	0.944	0.9979
2,3dinor-11β-PGF2α	0.015	0.045	0.110	0.330	0.9955
11β-PGF2α	0.058	0.174	0.254	0.762	0.9989
PGF2α	0.010	0.029	0.121	0.362	0.9968
PGE2	0.039	0.116	0.077	0.230	0.9994
11β-PGE2	0.036	0.108	0.147	0.442	0.9988
PGD2	0.156	0.467	0.294	0.881	0.9963
13,14-dihydro-15keto-PGF2α	0.157	0.470	0.041	0.122	0.9988

13,14-dihydro-PGF2α	0.121	0.364	0.042	0.126	0.9982
13,14-dihydro-15keto-PGE2	0.034	0.103	0.103	0.309	0.9973
13,14-dihydro-15keto-PGD2	0.084	0.251	0.149	0.447	0.9958
1a,1b-dihomo-PGF2α	0.019	0.056	0.045	0.135	0.9870
bicyclo-PGE2	0.027	0.081	0.010	0.029	0.9983
PGJ2	0.032	0.095	0.085	0.254	0.9948
PGK2	0.144	0.431	0.127	0.380	0.9980
PGA2	0.020	0.060	0.159	0.478	0.9968
15keto-PGF2α	0.030	0.091	0.083	0.249	0.9981
15deoxy-12,14-PGD2	0.040	0.121	0.114	0.341	0.9978
PGB2	0.024	0.072	0.076	0.228	0.9984
thromboxane-B2	0.005	0.016	0.744	2.231	0.9974
Oxylipin (Prostanoid)-EPA derived					
PGE3	0.017	0.051	0.190	0.569	0.9937
PGD3	0.113	0.340	0.203	0.608	0.9898
PGF3α	0.047	0.141	0.037	0.110	0.9929
PGA3	0.775	2.325	1.640	4.921	0.9976
thromboxane-B3	0.025	0.076	0.184	0.553	0.9984
Oxylipin (Leukotriene)-AA derived					
20-carboxy-LTB4	NA	NA	0.039	0.116	0.9935
20-hydroxy-LTB4	1.362	4.087	0.141	0.424	0.9936
6trans-LTB4	0.648	1.944	0.082	0.247	0.9984
LTB4	1.201	3.604	0.017	0.052	0.9992
LTB5	0.139	0.416	0.002	0.007	0.9964
14,15-LTE4	NA	NA	0.038	0.114	0.9910
LTE4	NA	NA	0.069	0.206	0.9975
11trans-LTE4	NA	NA	0.153	0.458	0.9980
Oxylipin (Resolvin)-EPA derived					
ResolvinE1	0.098	0.294	0.100	0.299	0.9982
Oxylipin (Resolvin)-DHA derived					
ResolvinD1	4.455	13.364	0.014	0.042	0.9974
ResolvinD2	1.262	3.787	0.084	0.252	0.9950
Oxylipin (Maresin)-DHA derived					
Maresin1	1.541	4.624	0.388	1.163	0.9963
Oxylipin (Lipoxin)-AA derived					
5S,6R-lipoxinA4	5.700	17.100	0.234	0.702	0.9959

5S,6S-lipoxinA4	2.055	6.164	0.233	0.700	0.9989
5S,14R-lipoxinB4	NA	NA	1.002	3.007	0.9973
Oxylipin (Lipoxin)-EPA derived					
LipoxinA5	0.102	0.306	0.063	0.190	0.9914
Oxylipin (Protectin)-DHA derived					
10,17-DiHDoHE	0.001	0.003	0.010	0.031	0.9915
Oxylipin (others)-LA derived					
9,10-EpOME	0.005	0.016	0.054	0.161	0.9928
12,13-EpOME	0.058	0.173	0.087	0.262	0.9969
9,10-DiHOME	0.176	0.529	1.345	4.036	0.9990
12,13-DiHOME	0.102	0.307	1.238	3.713	0.9987
9,10,13-TriHOME	0.185	0.554	0.145	0.436	0.9978
9,12,13-TriHOME	0.077	0.232	0.092	0.276	0.9971
9-HpODE	1.396	4.189	0.312	0.937	0.9959
13-HpODE	0.292	0.877	13.174	39.522	0.9893
9-HODE	0.344	1.032	2.339	7.018	0.9942
13-HODE	0.268	0.803	0.594	1.782	0.9918
9-KODE	0.333	0.998	0.150	0.451	0.9993
13-KODE	0.244	0.733	0.843	2.530	0.9857
Oxylipin (others)-MA derived					
5-HETrE	0.001	0.004	0.036	0.107	0.9849
Oxylipin (others)-DGLA derived					
8-HETrE	0.515	1.545	1.355	4.065	0.9973
15-HETrE	0.457	1.370	0.926	2.777	0.9985
Oxylipin (others)-AA derived					
12-HHTrE	0.399	1.197	0.179	0.536	0.9960
8,9-EpETrE	0.021	0.064	0.612	1.836	0.9997
11,12-EpETrE	0.004	0.012	0.004	0.013	0.9970
14,15-EpETrE	0.073	0.220	0.042	0.127	0.9960
5,6-DiHETrE	0.006	0.017	0.254	0.763	0.9969
8,9-DiHETrE	0.062	0.187	0.049	0.148	0.9968
11,12-DiHETrE	0.014	0.041	0.080	0.239	0.9996
14,15-DiHETrE	0.008	0.025	0.030	0.090	0.9990
12-HpETE	0.296	0.887	0.280	0.841	0.9971
15-HpETE	0.407	1.222	3.062	9.186	0.9919
5-HETE	0.070	0.211	0.099	0.296	0.9983

8-HETE	0.011	0.033	1.381	4.142	0.9980
9-HETE	0.027	0.080	0.023	0.069	0.9944
11-HETE	0.032	0.096	0.065	0.195	0.9915
12-HETE	0.049	0.146	2.771	8.312	0.9914
15-HETE	0.173	0.520	1.076	3.228	0.9945
20-HETE	0.015	0.046	0.248	0.745	0.9967
5-KETE	0.037	0.110	0.407	1.220	0.9868
12-KETE	0.247	0.741	0.388	1.164	0.9966
15-KETE	0.088	0.265	0.608	1.823	0.9905
5,15-DiHETE	0.180	0.540	2.800	8.400	0.9975
8,15-DiHETE	0.304	0.913	4.115	12.344	0.9841
Oxylipin (others)-ALA derived					
12,13-DiHODE	0.008	0.025	1.415	4.244	0.9991
9-HOTrE	0.491	1.474	0.523	1.570	0.9927
Oxylipin (others)-EPA derived					
5-HEPE	0.445	1.334	0.256	0.769	0.9934
9-HEPE	0.003	0.008	0.052	0.155	0.9896
12-HEPE	0.105	0.316	0.102	0.305	0.9946
15-HEPE	0.018	0.055	0.016	0.048	0.9872
18-HEPE	0.219	0.658	0.073	0.220	0.9967
14,15-EpETE	0.007	0.020	0.120	0.359	0.9894
17,18-EpETE	0.062	0.185	0.002	0.006	0.9957
14,15-DiHETE	0.026	0.077	0.038	0.114	0.9989
17,18-DiHETE	0.096	0.287	0.051	0.153	0.9976
Oxylipin (others)-DHA derived					
16,17-EpDPE	0.137	0.411	0.072	0.216	0.9945
19,20-EpDPE	0.018	0.053	0.052	0.157	0.9973
19,20-DiHDPA	0.004	0.012	0.010	0.031	0.9983
4-HDoHE	0.040	0.121	0.146	0.437	0.9815
7-HDoHE	0.022	0.066	0.167	0.501	0.9846
8-HDoHE	0.001	0.003	0.010	0.031	0.9944
10-HDoHE	0.046	0.138	0.431	1.294	0.9974
11-HDoHE	0.005	0.014	0.147	0.441	0.9954
13-HDoHE	0.027	0.080	0.557	1.671	0.9887
14-HDoHE	0.062	0.186	0.074	0.221	0.9940
16-HDoHE	0.003	0.008	0.072	0.216	0.9945

17-HDoHE	0.010	0.031	0.057	0.172	0.9838
20-HDoHE	0.010	0.029	0.385	1.154	0.9935
Bile acid and cortisol					
GUDCA	0.921	2.764	9.030	27.091	0.9877
GCA	0.00008	0.00024	27.366	82.097	0.9950
CA	1.338	4.013	3.715	11.144	0.9982
GCDCA	0.788	2.365	69.570	208.711	0.9975
GDCA	15.209	45.627	47.226	141.678	0.9973
CDCA	0.489	1.467	5.393	16.179	0.9956
DCA	1.036	3.107	17.294	51.881	0.9923
GLCA	0.662	1.986	2.064	6.192	0.9965
TUDCA	0.380	1.140	0.974	2.921	0.9955
THDCA	0.000	0.001	0.115	0.346	0.9985
TCDCA	0.286	0.857	3.334	10.003	0.9969
TDCA	0.495	1.486	2.243	6.728	0.9968
TCA	0.023	0.069	1.510	4.531	0.9968
TLCA	0.033	0.100	0.563	1.688	0.9988
TLCA-3S	0.488	1.465	4.338	13.013	0.9924
LCA	2.199	6.597	2.564	7.691	0.9951
UDCA	16.845	50.535	1.641	4.922	0.9908
Cortisol	0.553	1.660	0.413	1.239	0.9981
Endocannabinoid					
α-LEA	0.281	0.843	0.143	0.428	0.9954
POEA	0.645	1.936	0.232	0.696	0.9915
PDEA	0.032	0.095	0.054	0.162	0.9939
LEA	0.607	1.820	0.180	0.540	0.9941
AEA	0.113	0.339	0.034	0.101	0.9884
DHEA	0.011	0.032	0.044	0.131	0.9920
1-AG & 2-AG	0.172	0.515	0.711	2.133	0.9931
1-LG & 2-LG	6.862	20.585	165.259	495.778	0.9887
PEA	1.418	4.255	1.244	3.731	0.9916
DGLEA	0.009	0.027	0.017	0.050	0.9983
2-AGE	0.052	0.157	0.107	0.321	0.9978
DEA	0.036	0.108	0.086	0.258	0.9974
1-OG & 2-OG	5.737	17.212	80.299	240.898	0.9824
SEA	0.147	0.440	1.240	3.719	0.9948

NADA	0.128	0.384	0.446	1.338	0.9986
OEA	0.687	2.060	0.129	0.388	0.9947
EPEA	0.003	0.008	0.020	0.060	0.9861
ETAEA	0.016	0.049	0.081	0.242	0.9935

Table S4. Concentrations of each metabolite measured in NIST SRM 1950 and human pooled plasma

Compound	**Concentration in pooled human plasma (nM)**	**Concentration in NIST SRM 1950 (nM)**
Sphingoid base		
Sphinganine C18:0	4.08	6.665
Sphingosine C18:1	22	44
Sphinganine-1-phosphate C18:0	31	61
Sphingosine-1-phosphate C18:1	166	364
Lysophospholipid		
LPA C16:0	3302	521
LPA C18:0	370	140
LPA C18:1	339	95
LPA C20:4	779	257
cLPA C18:1	446	55
LPE C18:1	2578	1770
LPG C18:1	54	57
LPS C18:1	46	3.716
LPI C20:4 [b]	64	65
Platelet Activating Factor		
PAF C16:0	NA	NA
Free fatty acid		
FA C18:1 w9 (OA)		
FA C18:2 w6 (LA)		
FA C18:3 w3 (ALA)		
FA C18:3 w6 (GLA)		
FA C20:3 w6 (DGLA)		
FA C20:3 w9 (MA)		

FA C20:4 w6 (AA)		
FA C20:5 w3 (EPA)		
FA C22:4 w6 (ADA)		
FA C22:6 w3 (DHA)		
Nitro fatty acid		
NO_2-LA	0.625	0.603
NO_2-OA	0.127	1.433
Oxylipin (Isoprostane)-DGLA derived		
8-iso-PGA1	0.942	0.375
8-iso-PGE1	0.292	NA
Oxylipin (Isoprostane)-AA derived		
2,3dinor-8-iso-PGF2α	NA	NA
8-iso-15R-PGF2α	0.713	NA
8-iso-PGF2α	0.524	NA
8-iso-PGE2	1.936	NA
5-iPF2α-VI	4.833	0.446
8,12-iso-iPF2α-VI	28	4.68
8-iso-13,14-dihydro-15keto-PGF2α	NA	NA
8-iso-PGA2	0.223	0.03
8-iso-15keto-PGE2	8.698	NA
8-iso-15keto-PGF2β	0.672	0.375
8-iso-15keto-PGF2α	0.43	NA
Oxylipin (Isoprostane)-EPA derived		
8-iso-PGF3α	NA	NA
Oxylipin (Prostanoid)-DGLA derived		
PGA1	0.426	NA
PGE1	1.489	0.032
PGF1α	NA	NA
13,14-dihydro-15keto-PGF1α	NA	NA
6-keto-PGF1α	0.671	0.636
13,14-dihydro-15keto-PGD1	NA	NA
thromboxane-B1	NA	NA
Oxylipin (Prostanoid)-AA derived		
20-hydroxy-PGF2α	NA	NA
20-hydroxy-PGE2	NA	NA
2,3dinor-11β-PGF2α	NA	NA

11β-PGF2α	1.119	1.527
PGF2α	0.628	0.102
PGE2 [b]	2.685	0.049
11β-PGE2	1.291	NA
PGD2 [b]	9.513	0.463
13,14-dihydro-15keto-PGF2α	NA	NA
13,14-dihydro-PGF2α	1.205	NA
13,14-dihydro-15keto-PGE2	NA	NA
13,14-dihydro-15keto-PGD2	2.115	NA
1a,1b-dihomo-PGF2α	0.698	NA
bicyclo-PGE2	0.946	NA
PGJ2	0.687	NA
PGK2	NA	NA
PGA2	0.593	0.038
15keto-PGF2α	0.413	NA
15deoxy-12,14-PGD2	0.418	NA
PGB2	9.614	NA
thromboxane-B2	1.609	0.31
Oxylipin (Prostanoid)-EPA derived		
PGE3	NA	NA
PGD3	0.051	NA
PGF3α	NA	NA
PGA3	NA	NA
thromboxane-B3	NA	NA
Oxylipin (Leukotriene)-AA derived		
20-carboxy-LTB4	0.061	0.039
20-hydroxy-LTB4	NA	NA
6trans-LTB4	22	1.381
LTB4	0.455	0.059
LTB5	0.356	NA
14,15-LTE4	NA	NA
LTE4	NA	0.079
11trans-LTE4	NA	NA
Oxylipin (Resolvin)-EPA derived		
ResolvinE1	0.426	NA
Oxylipin (Resolvin)-DHA derived		

ResolvinD1	0.406	NA
ResolvinD2	NA	NA
Oxylipin (Maresin)-DHA derived		
Maresin1	2.887	NA
Oxylipin (Lipoxin)-AA derived		
5S,6R-lipoxinA4	6.837	1.162
5S,6S-lipoxinA4	1.843	NA
5S,14R-lipoxinB4	9.495	2.005
Oxylipin (Lipoxin)-EPA derived		
LipoxinA5	0.048	NA
Oxylipin (Protectin)-DHA derived		
10,17-DiHDoHE	2.737	0.007
Oxylipin (others)-LA derived		
9,10-EpOME [b]	1.226	1.122
12,13-EpOME	1.181	1.477
9,10-DiHOME	7.193	5.826
12,13-DiHOME	9.534	4.285
9,10,13-TriHOME	3.608	1.561
9,12,13-TriHOME	3.877	1.968
9-HpODE	9.859	NA
13-HpODE	NA	NA
9-HODE	132	8.152
13-HODE [b]	138	11
9-KODE	4.983	6.216
13-KODE	1.527	1.365
Oxylipin (others)-MA derived		
5-HETrE	7.933	0.13
Oxylipin (others)-DGLA derived		
8-HETrE	9.672	NA
15-HETrE	4.292	NA
Oxylipin (others)-AA derived		
12-HHTrE	3.15	0.325
8,9-EpETrE	3.554	NA
11,12-EpETrE	0.138	0.018
14,15-EpETrE	0.399	NA
5,6-DiHETrE	3.309	0.95

8,9-DiHETrE [b]	0.979	0.386
11,12-DiHETrE	0.599	0.526
14,15-DiHETrE [b]	0.7	0.769
12-HpETE	NA	NA
15-HpETE	NA	NA
5-HETE	233	7.732
8-HETE	28	NA
9-HETE	30	0.413
11-HETE [b]	30	0.462
12-HETE	31	5.167
15-HETE	23	1.734
20-HETE	1.046	1.185
5-KETE	1.089	0.063
12-KETE	6.011	NA
15-KETE	4.521	NA
5,15-DiHETE	32	0.529
8,15-DiHETE	71	NA
Oxylipin (others)-ALA derived		
12,13-DiHODE	8.227	2.77
9-HOTrE	0.545	0.044
Oxylipin (others)-EPA derived		
5-HEPE	2.297	0.516
9-HEPE	0.682	0.219
12-HEPE [b]	1.028	0.244
15-HEPE [b]	0.838	0.258
18-HEPE	0.304	NA
14,15-EpETE	0.016	NA
17,18-EpETE	NA	NA
14,15-DiHETE	NA	0.438
17,18-DiHETE	1.349	1.098
Oxylipin (others)-DHA derived		
16,17-EpDPE	0.259	NA
19,20-EpDPE	1.867	0.167
19,20-DiHDPA	0.723	1.011
4-HDoHE	29	1.283
7-HDoHE	3.284	0.966

8-HDoHE [b]	5.159	NA
10-HDoHE	3.751	NA
11-HDoHE	8.398	0.019
13-HDoHE	15	0.074
14-HDoHE	11	0.292
16-HDoHE	5.705	0.081
17-HDoHE	34	0.338
20-HDoHE	3.614	NA
Bile acid and cortisol		
GUDCA	226	226
GCA	374	239
CA	126	130
GCDCA	1382	1368
GDCA	429	475
CDCA	357	340
DCA	437	576
GLCA	15	22
TUDCA	7.867	4.474
THDCA	0.339	0.227
TCDCA	208	105
TDCA	80	41
TCA	94	25
TLCA	3.069	2.161
TLCA-3S	209	105
LCA	4.196	12
UDCA	53	135
Cortisol	235	272
Endocannabinoid		
α-LEA	1.043	2.552
POEA	0.449	0.752
PDEA [a]	0.356	0.38
LEA	5.546	8.984
AEA	0.73	1.138
DHEA	1.402	2.828
1-AG & 2-AG	49	104
1-LG & 2-LG	543	1682

PEA [a]	4.823	9.713
DGLEA	0.025	0.05
2-AGE	NA	NA
DEA	0.228	0.475
1-OG & 2-OG	1758	3346
SEA [a]	4.858	9.128
NADA	NA	NA
OEA	12	26
EPEA	NA	NA
ETAEA	NA	NA

Measured concentrations of each metabolite are mean values calculated from technical replicates and with S/N higher than 3 if the value is lower than LOD.

NA: Metabolite without detected peak or peak intensity too low for accurate quantitation.

[a] Metabolite with caution, relatively higher background in blank sample.

[b] Metabolite with coefficient of dispersion (COD) values higher than 40% across labs.

Table S5. Metabolite concentrations in NIST SRM 1950: measured concentrations, certified concentrations and reported concentrations.(Supplementary data for Figure 5)

Compound	Measured con. in NIST (nM)	Certified con. in NIST (nM)	Reported con. in NIST (nM)
Sphingoid base			
Sphinganine-1-phosphate C18:0	61	100	NA
Sphingosine-1-phosphate C18:1	364	410	NA
Lysophospholipid			
LPE C18:1	1770	1400	NA
Oxylipin (Prostanoid)-AA derived			
PGE2	0.049	0.040	0.140
Oxylipin (Leukotriene)-AA derived			
LTB4	0.059	0.030	NA
Oxylipin (others)-LA derived			
12,13-EpOME	1.477	7.800	4.080
9,10-DiHOME	5.826	7.000	4.390
12,13-DiHOME	4.285	5.000	3.640
9-HODE	8.152	9.700	9.000
9-KODE	6.216	6.800	NA
Oxylipin (others)-MA derived			
5-HETrE	0.130	1.200	NA
Oxylipin (others)-AA derived			
12-HHTrE	0.325	0.270	NA
5,6-DiHETrE	0.950	1.500	1.350
11,12-DiHETrE	0.526	1.000	NA
5-HETE	7.732	10	11.500
9-HETE	0.413	0.850	0.811
12-HETE	5.167	6.800	8.310
15-HETE	1.734	2.400	2.340
20-HETE	1.185	2.000	NA
5-KETE	0.063	0.480	NA
5,15-DiHETE	0.529	0.250	0.467
Oxylipin (others)-EPA derived			
5-HEPE	0.516	0.860	0.952
9-HEPE	0.219	0.500	0.159
Oxylipin (others)-DHA derived			
19,20-DiHDPA	1.011	1.600	1.300
4-HDoHE	1.283	3.900	2.390

11-HDoHE	0.019	0.610	NA
14-HDoHE	0.292	1.300	3.440
17-HDoHE	0.338	0.840	NA
Bile acid and cortisol			
GUDCA	226	150	242
GCA	239	240	279
CA	130	120	163
GCDCA	1368	1100	1480
GDCA	475	430	543
CDCA	340	300	452
DCA	576	350	491
GLCA	22	25	89
TCDCA	105	84	106
TDCA	41	40	45
TCA	25	26	26
TLCA	2.161	2.700	2.030
TLCA-3S	105	100	NA
LCA	12	14	19
UDCA	135	110	172
Cortisol	272	231	258
Endocannabinoid			
α-LEA	2.552	NA	0.121
LEA	8.984	NA	3.400
AEA	1.138	NA	1.360
DHEA	2.828	NA	0.643
1-AG & 2-AG	104	NA	124
1-LG & 2-LG	1682	NA	1890
DGLEA	0.050	NA	0.144
DEA	0.475	NA	0.402
1-OG & 2-OG	3346	NA	3000
OEA	25.808	NA	3.970